FIFTH CERN-FERMILAB HADRON COLLIDER PHYSICS SUMMER SCHOOL

August 16-27, 2010

PARTICLE IDENTIFICATION

OLAV ULLALAND (CERN)

Mainly nuts and bolts and how they could fit together.

When the messenger goes faster than the message:

Particle Identification with **Cherenkov Radiation**.

Observation of Antiprotons*

OWEN CHAMBERLAIN, EMILIO SEGRÈ, CLYDE WIEGAND, AND THOMAS YPSILANTIS

Radiation Laboratory, Department of Physics, University of California, Berkeley, California

(Received October 24, 1955)

The most legendary experiment built on PID with Cherenkov radiation.

OWEN CHAMBERLAIN

The early antiproton work

Nobel Lecture, December 11, 1959

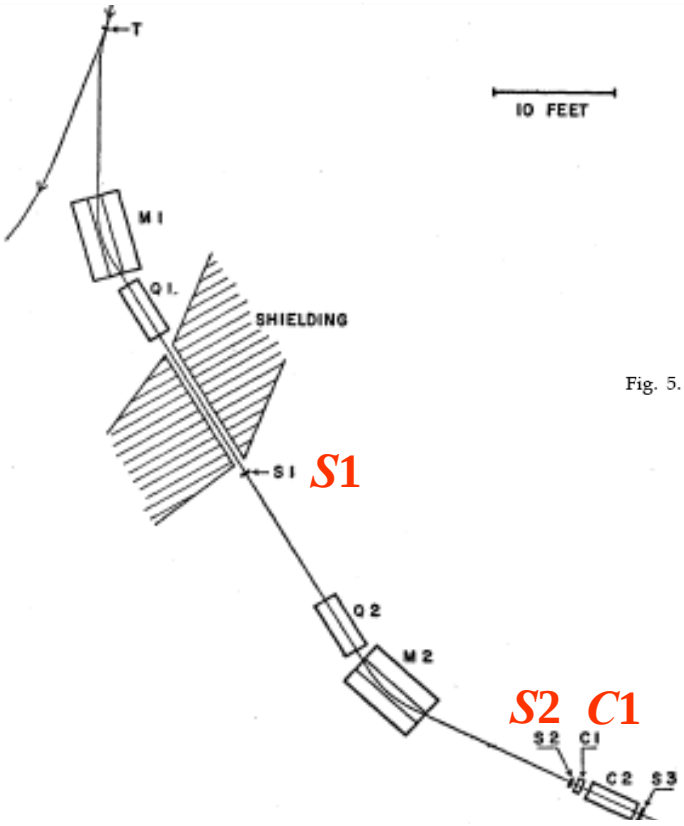

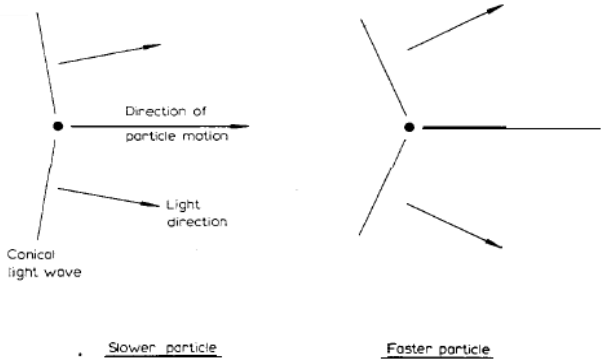

Fig. 5. Diagram of Čerenkov radiation. The angle of emission of Čerenkov depends on the speed of the charged particle.

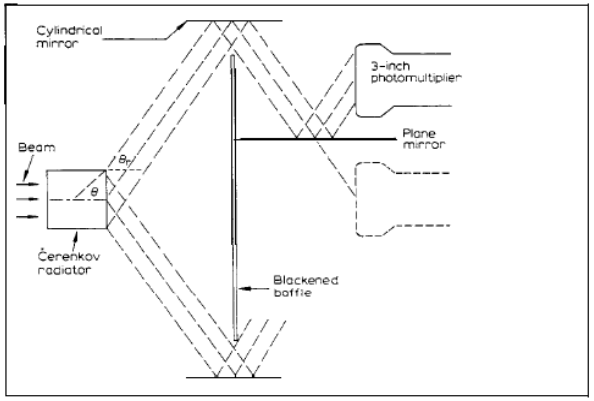

Velocity-selecting Čerenkov counter (C 27)

Fig. 7. View of the velocity-selecting Čerenkov counter.

TABLE I. Characteristics of components of the apparatus.

*S*1, *S*2	Plastic scintillator counters 2.25 in. diameter by 0.62 in. thick.
*C*1	Čerenkov counter of fluorochemical 0–75, ($C_8F_{16}O$); $\mu_D = 1.276$; $\rho = 1.76$ g cm^{-3}. Diameter 3 in.; thickness 2 in.
*C*2	Čerenkov counter of fused quartz: $\mu_D = 1.458$; $\rho = 2.2$ g cm^{-3}. Diameter 2.38 in.; length 2.5 in.
*Q*1, *Q*2	Quadrupole focusing magnets: Focal length 119 in.; aperture 4 in.
*M*1, *M*2	Deflecting magnets 60 in. long. Aperture 12 in. by 4 in. $B \cong 13\,700$ gauss.

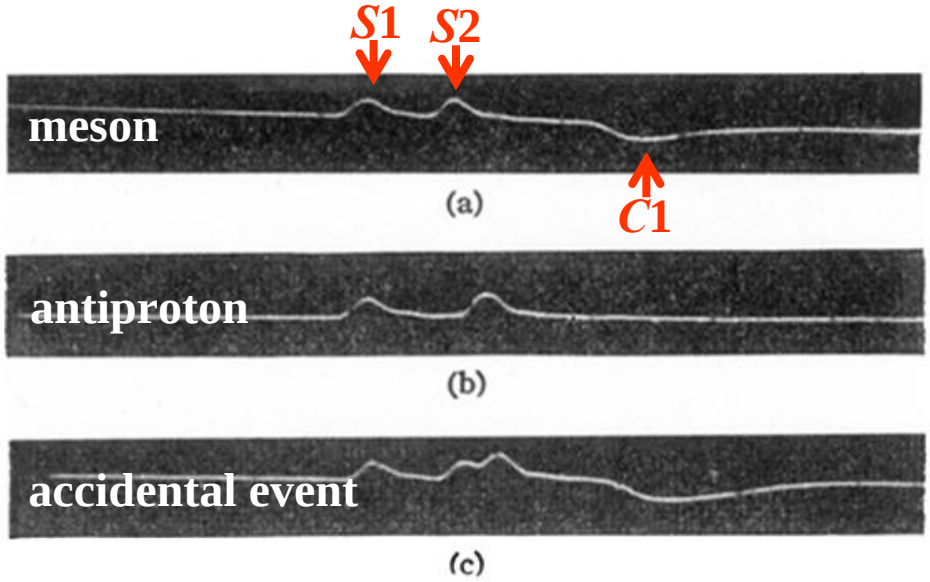

FIG. 2. Oscilloscope traces showing from left to right pulses from *S*1, *S*2, and *C*1. (a) meson, (b) antiproton, (c) accidental event.

The Cherenkov radiation condition:

ε real ✓

and

$0 \le \cos(\Theta) \le 1$ ✓

$$\cos\Theta_C = \frac{1}{\beta \cdot n}$$

where n is the refractive index

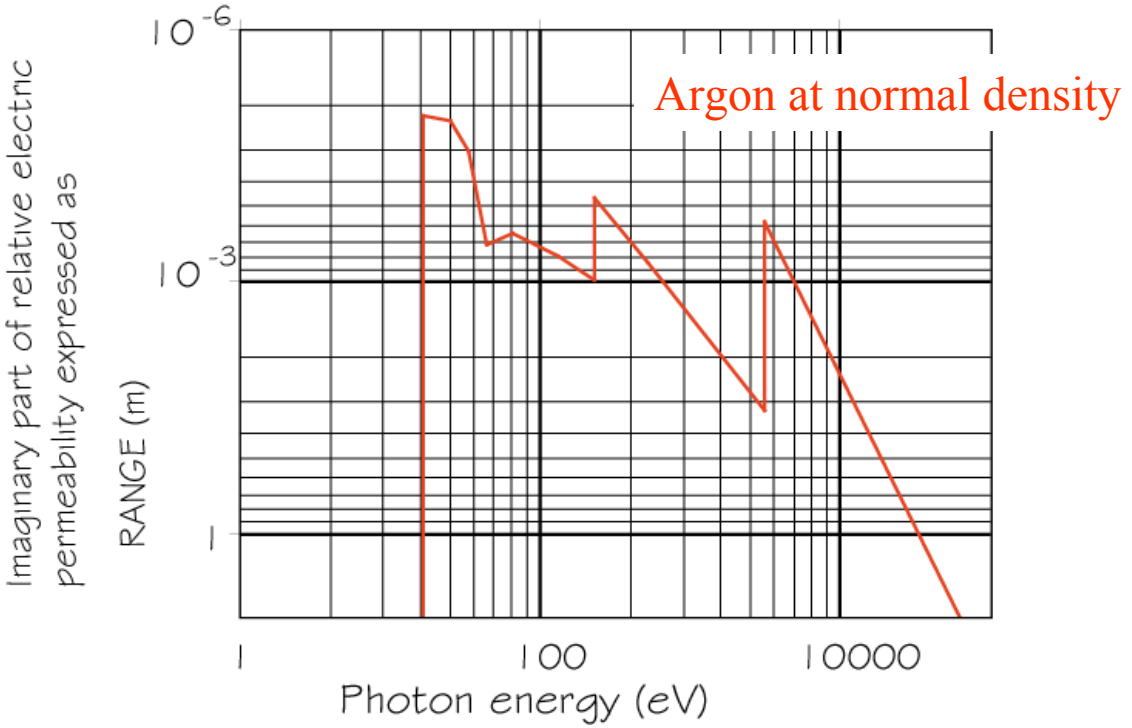

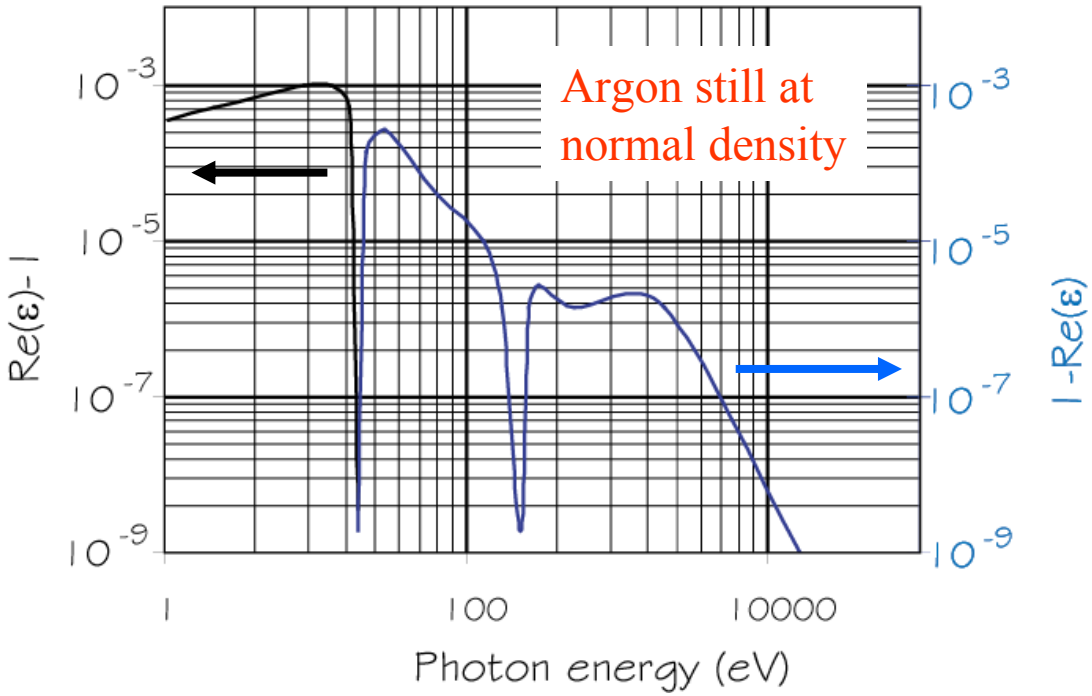

W.W.M. Allison and P.R.S. Wright, RD/606-2000-January 1984

Some words on refractive index

The normal way to express n is as a power series.
For a simple gas, a simple
one pole Sellmeier approximation:

$$(n-1)\cdot 10^6 = \frac{0.05085}{\left(\frac{1}{73.8}\right)^2 - \left(\frac{1}{\lambda(nm)}\right)^2}$$

Argon

$=16.8$ eV

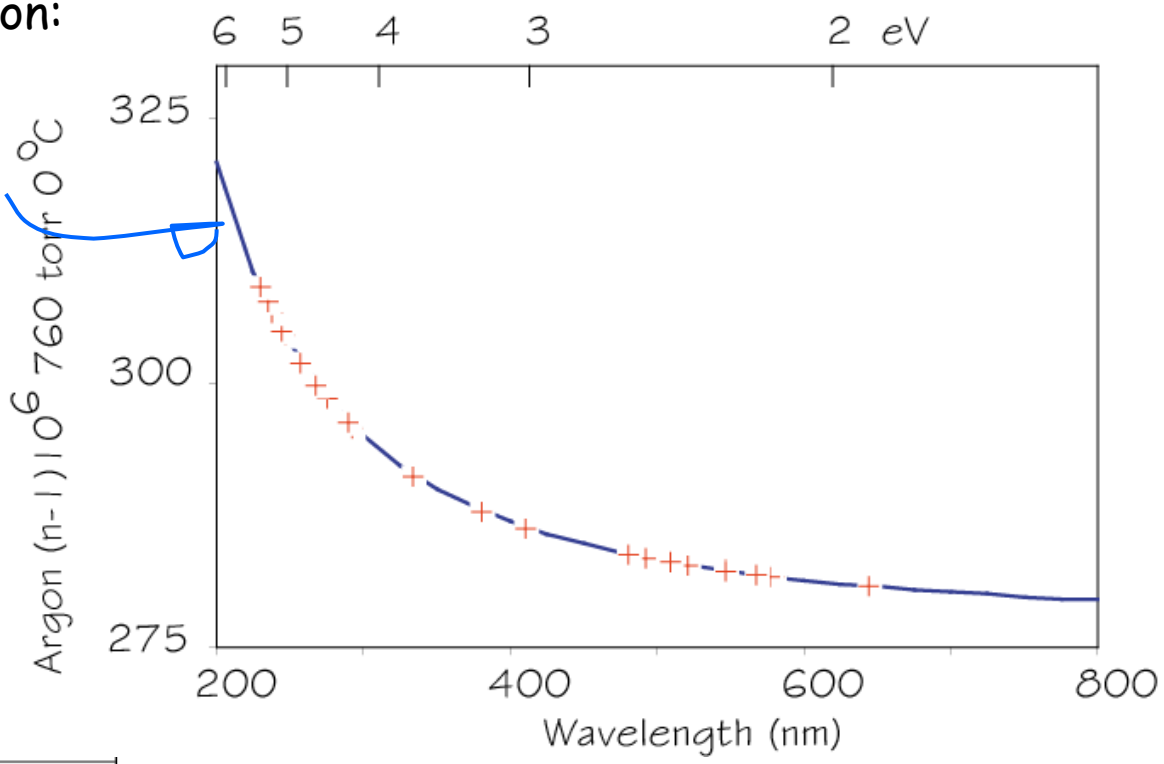

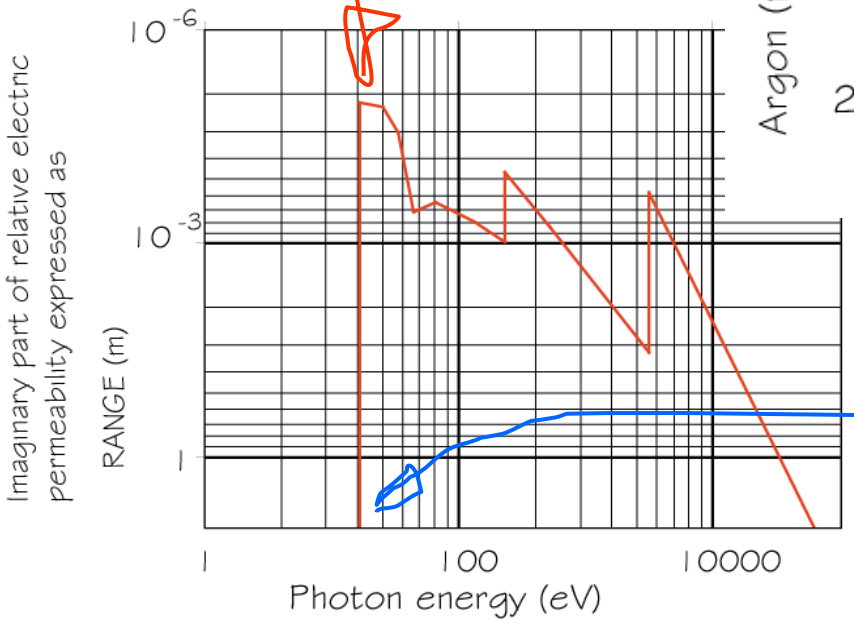

$\Rightarrow$ ω_0^2=(plasma frequency) ^{2}
$\propto$ (electron density)

For more on the plasma frequency, try Jackson, Section 7 (or similar)
or go to sites like
http://farside.ph.utexas.edu/teaching/plasma/lectures/node44.html

$$n-1=\frac{A}{\lambda_0^{-2}-\lambda^{-2}}$$

$$\frac{dN_{ph}}{dLd\lambda}=2\pi\alpha Z^2\frac{1}{\lambda^2}\sin^2\Theta$$

$$\cos\Theta=\frac{1}{\beta n}$$

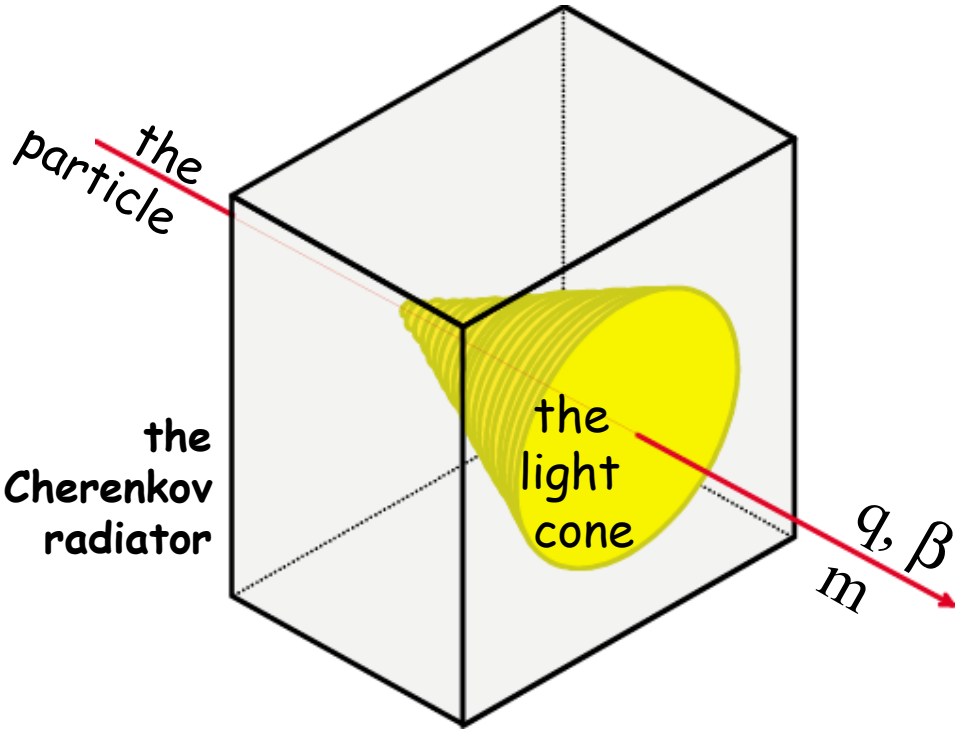

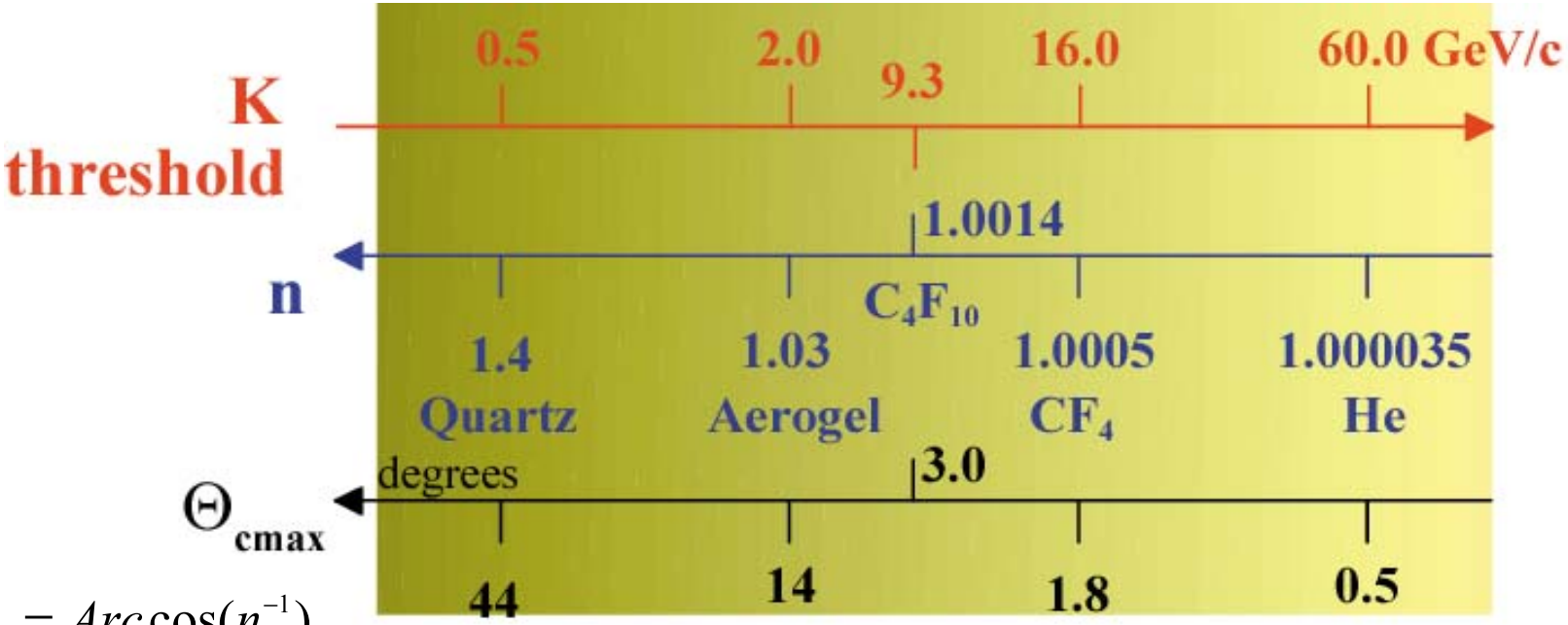

$$\Theta_{C\max}=Arc\cos(n^{-1})$$

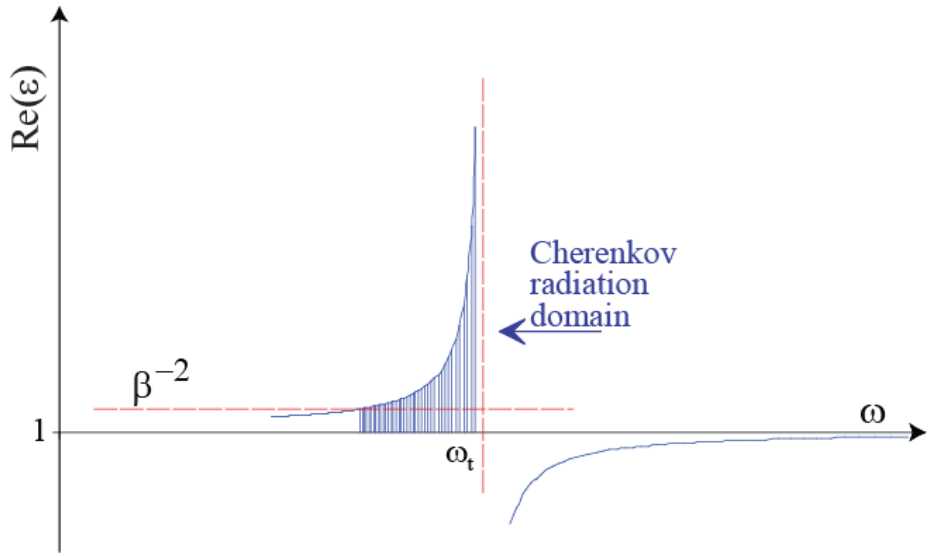

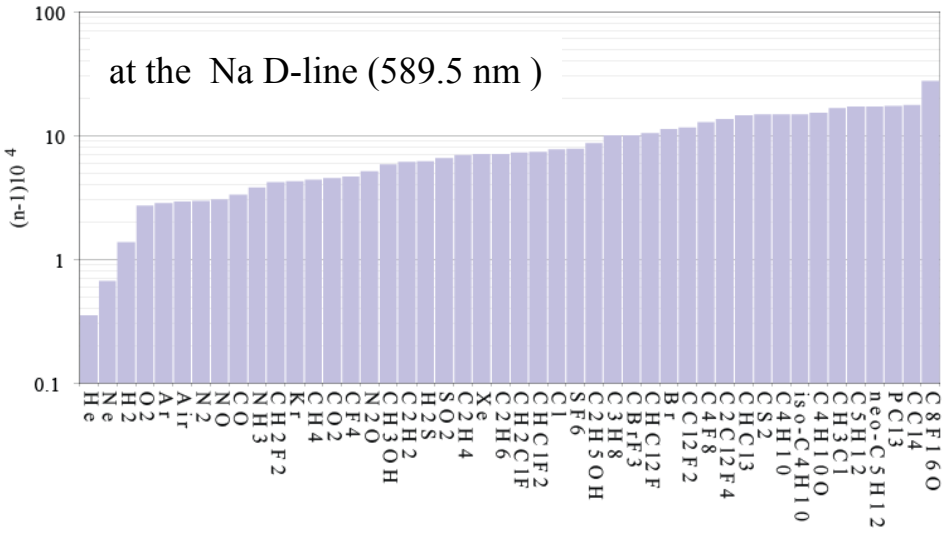

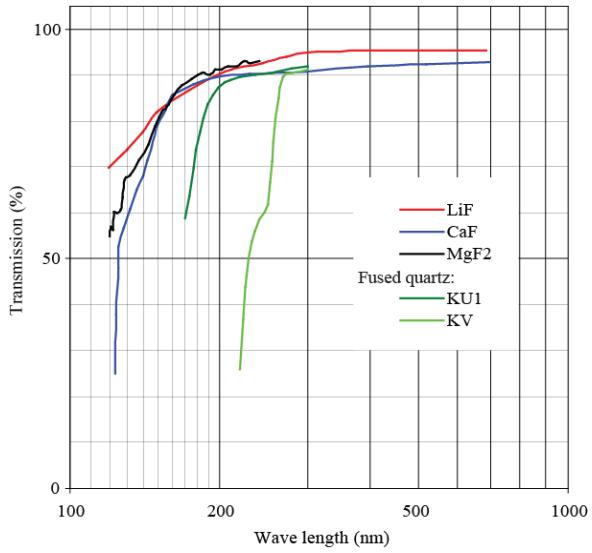

Photon absorption in quartz

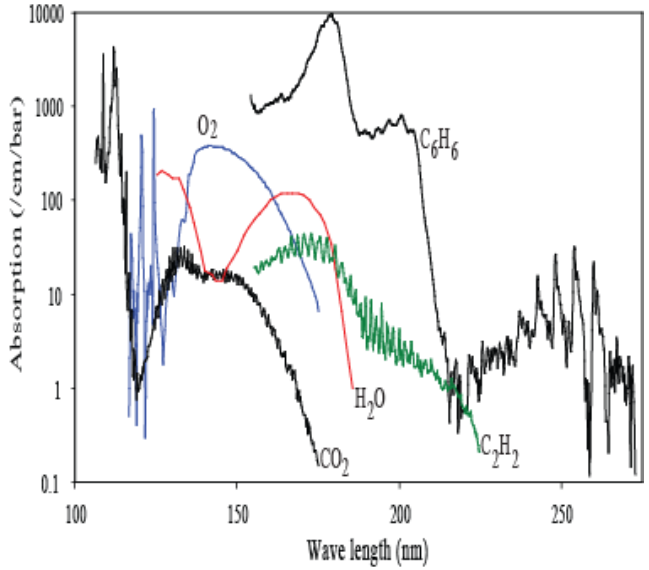

Photon absorption in gases.

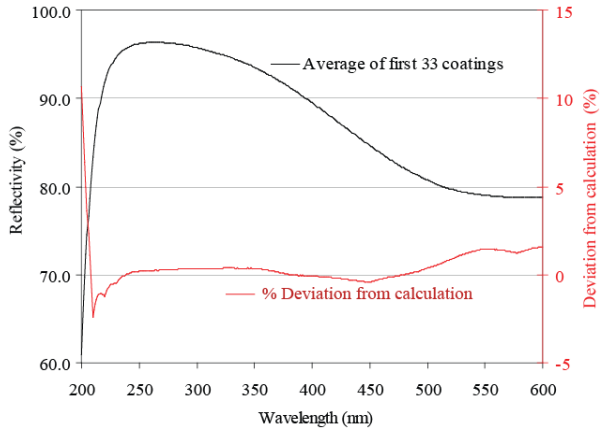

Mirror reflectivity

and then there is the photon detector.

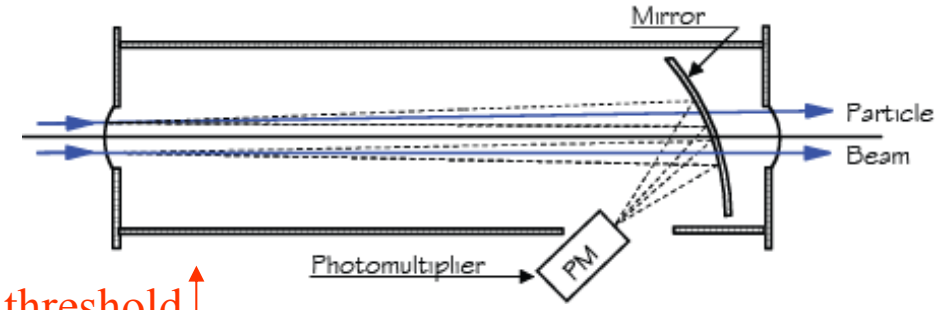

threshold

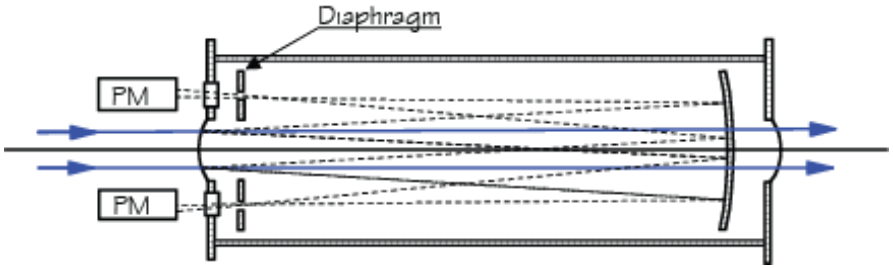

differential

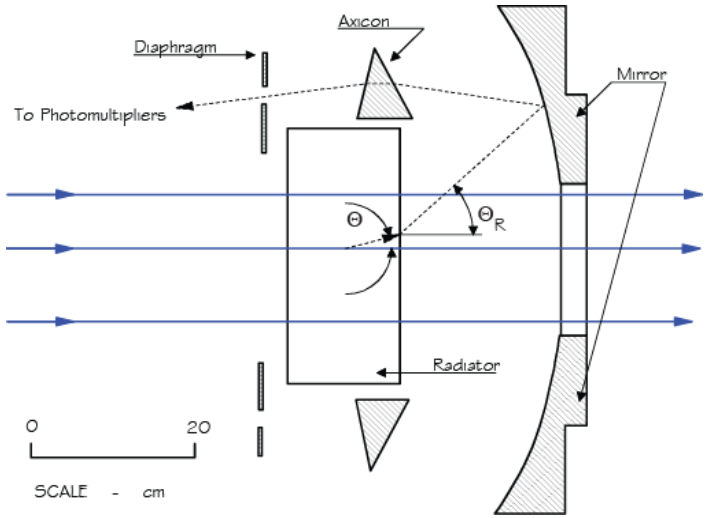

achromatic

B radiator: n=1.0003

A radiator: n=1.0024

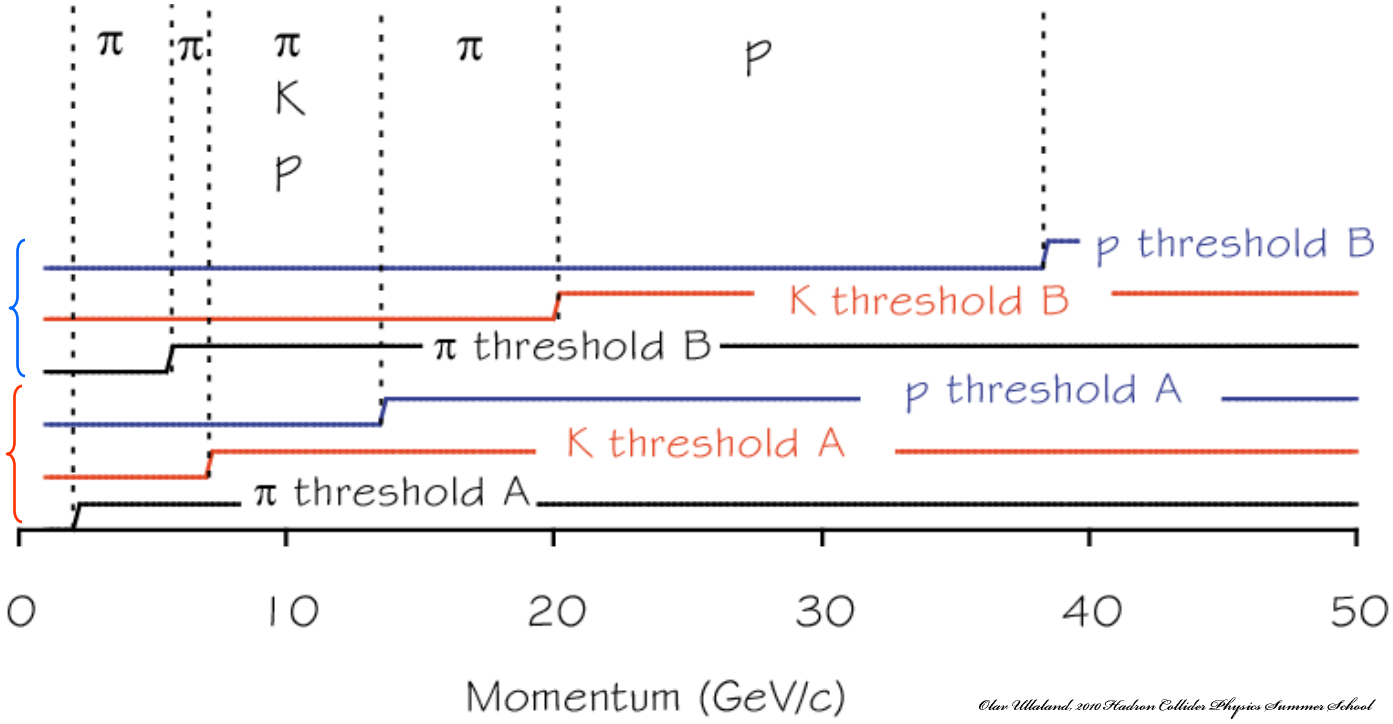

Use all available information about the Cherenkov radiation:

- The existence of a threshold
- The dependence of the number of photons
- The dependence of Cherenkov angle on the velocity $\beta = p/E$ of the particle
- The dependence on the charge of the particle

+

Capability to do single photon detection

- with high efficiency
- with high space resolution

⇒ Ring Imaging Cherenkov detector

the RICH

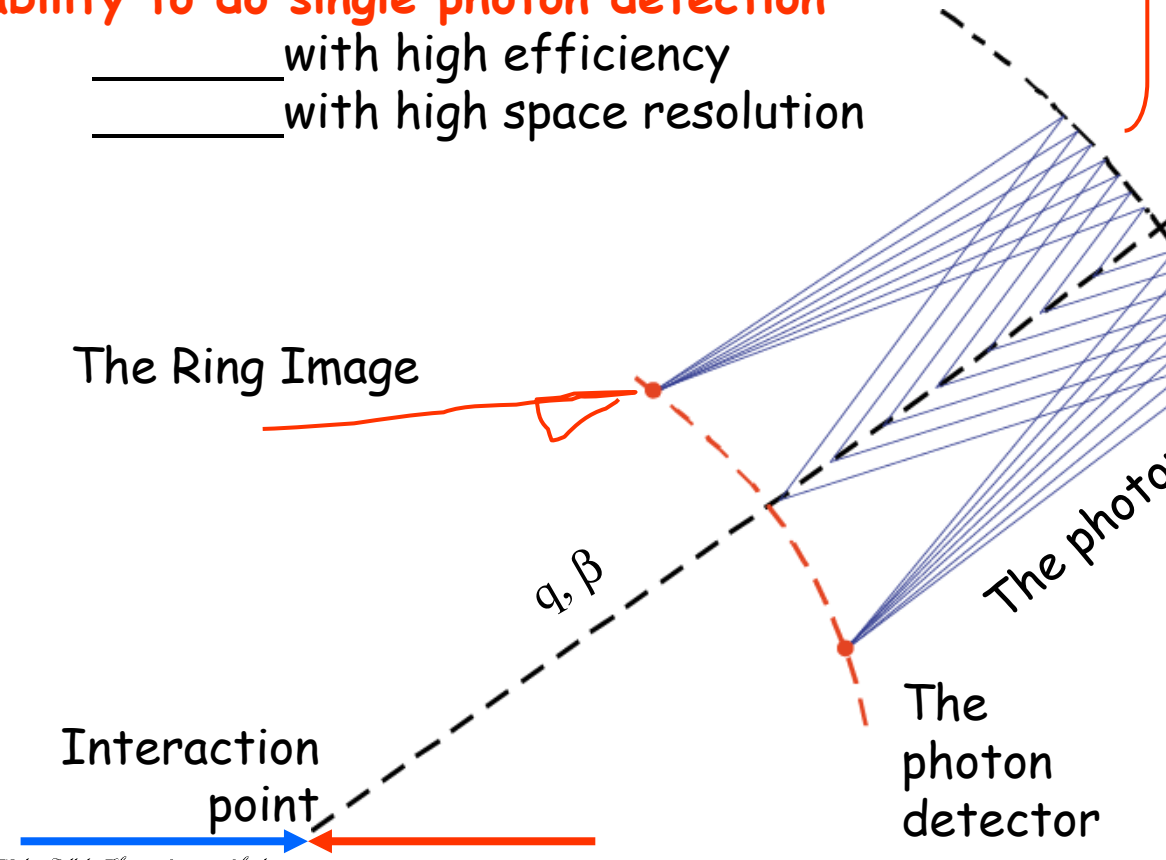

The beginning:
J. Seguinot and T. Ypsilantis, Photo-ionisation and Cherenkov ring imaging, Nucl. Instr. and Meth. 142(1977)377


http://veritas.sao.arizona.edu/

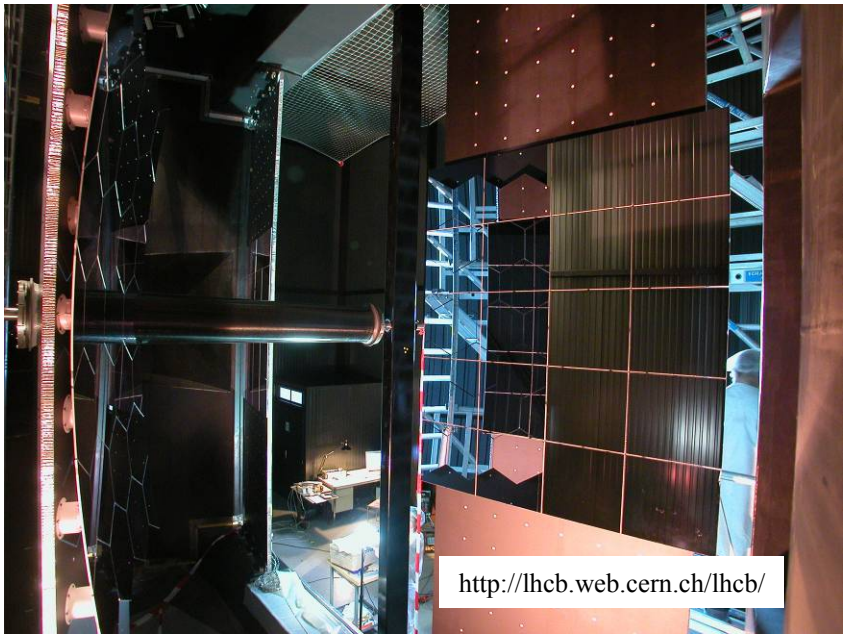
http://lhcb.web.cern.ch/lhcb/


http://wwwcompass.cern.ch/

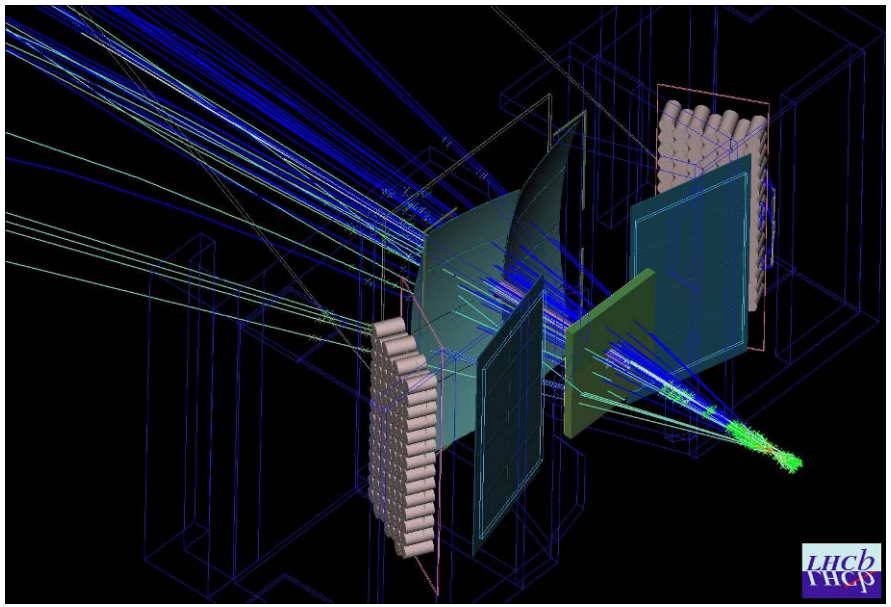
LHCb

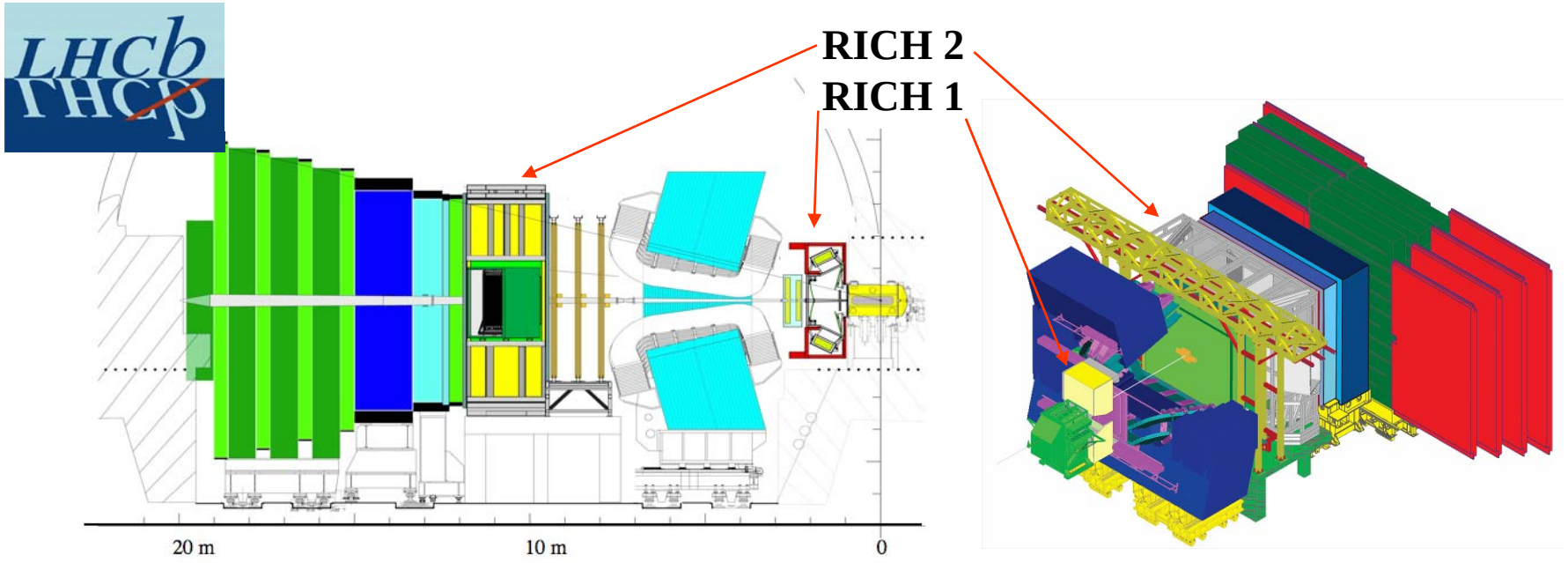
RICH 2
RICH 1
20 m
10 m
0

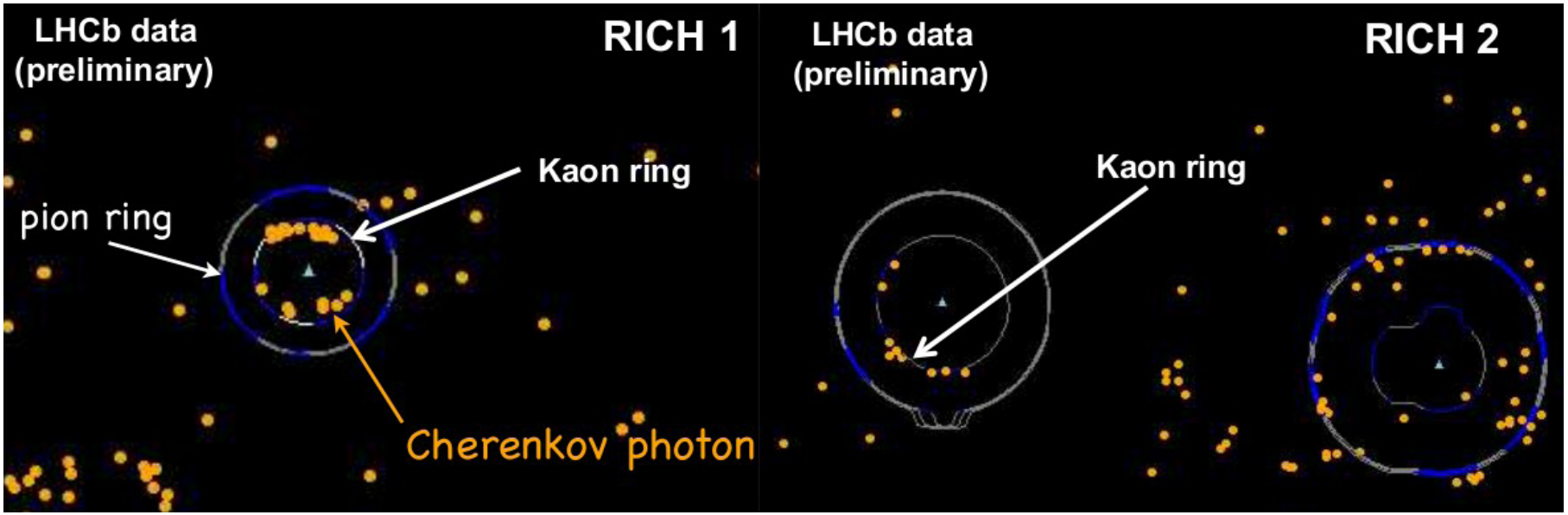
LHCb data
(preliminary)
RICH 1
Kaon ring
pion ring
Cherenkov photon
LHCb data
(preliminary)
RICH 2
Kaon ring

From Photons ⇒ Hits ⇒ Rings.

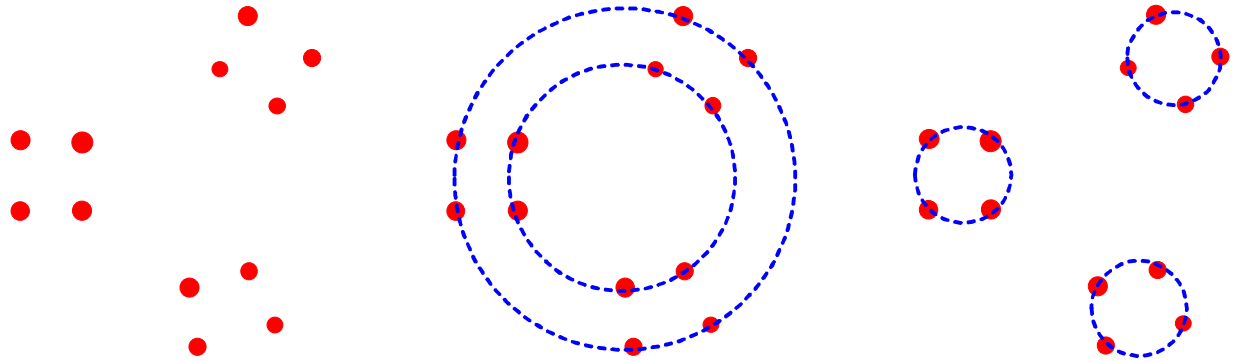

(a) (b) (c)

There is no way to recognise a pattern if one does not know what one is looking for!

What rings should we see in (a)?

Are there two large concentric rings as indicated in (b)?

Perhaps there are three small rings of equal radii as indicated in (c).

The answer *must* depend on what rings we expect to see!

Equivalently, the answer *must* depend on the process which is believed to have lead to the dots being generated in the first place. If we were to know *without doubt* that the process which generated the rings which generated the dots in (a) were only capable of generating large concentric rings, then only (b) is compatible with (a). If we were to know *without doubt* that the process were only capable of making small rings, then (c) is the only valid interpretation. If we know the process could do either, then both (b) and (c) might be valid, though one might be more likely than the other depending on the relative probability of each being generated. Finally, if we were to know that the process only generated *tiny* rings, then there is yet another way of interpreting (a), namely that it represents 12 *tiny* rings of radius too small to see.

from C.G. Lester, NIM 560(2006)621

Doom
Gloom
and
Despair

as in

inAccuracy
unCertainty
misCalculation
imPerfection
inPrecision

or plain

blunders
errors and
faults.

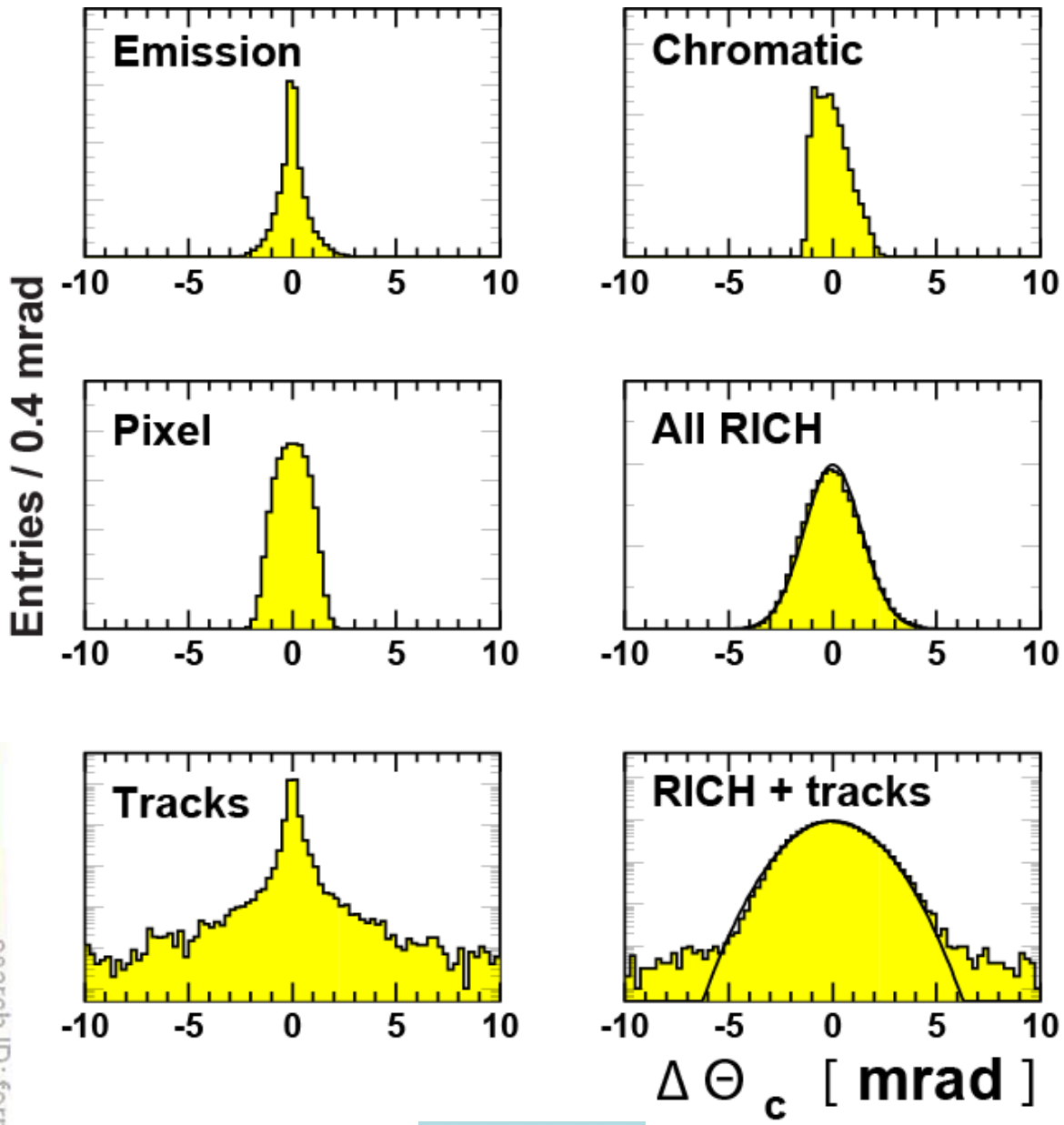

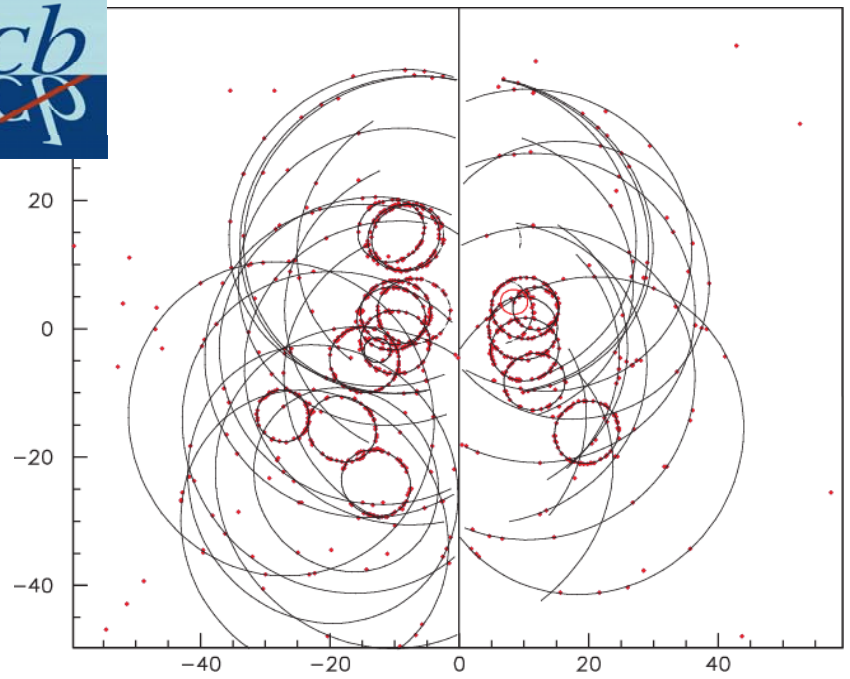

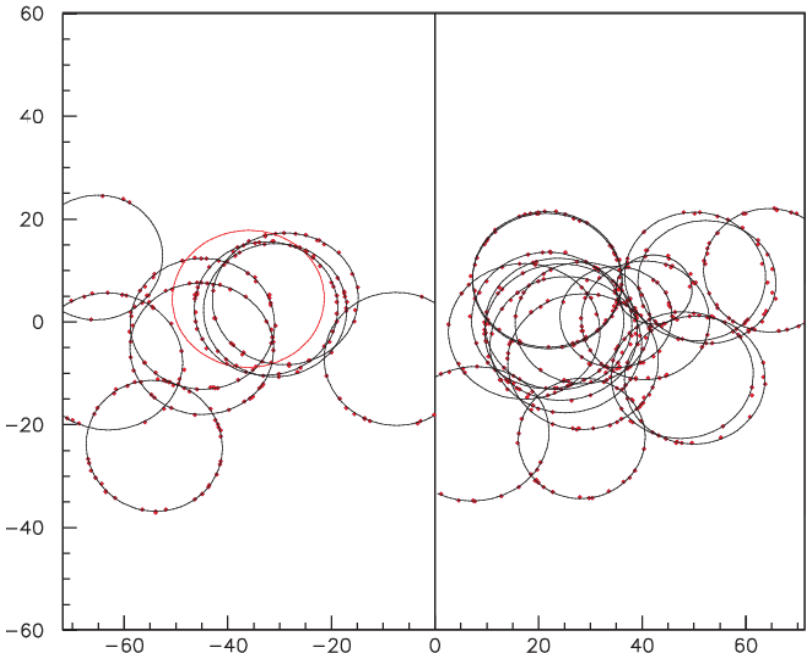

Local analysis:_____
Each track is taken in turn.

$$\ln \mathcal{L} = \sum_i \ln\left(1 + \frac{1}{\sqrt{2\pi}\sigma_\Theta \kappa} \exp\left[-\frac{(\Theta_i - \Theta_x)^2}{2\sigma_\Theta^2}\right]\right)$$

Θ_i : calculated emission angle for hit i
Θ_x : expected angle for hypothesis x
σ_Θ: angular resolution
κ: hit selection parameter

Global analysis:_____
The likelihood is constructed for the whole event:

$$\ln \mathcal{L} = -\sum_{\text{track } j} \mu_j + \sum_{\text{pixel } i} n_i \ln\left(\sum_{\text{track } j} a_{ij} + b_i\right)$$

a_{ij}: expected hits from track j in detector/pixel i
$\mu_j = \Sigma_i a_{ij}$
n_i: hits in detector i
b_i: expected background in detector i

Putting some meat to these bare bones.

Will follow R. Forty and O. Schneider, RICH pattern recognition, LHCB/98-40

C.P. Buszello, LHCB RICH pattern recognition and particle identification performance, NIM A 595(2008) 245-247

Cherenkov angle reconstruction:

reconstructing the Cherenkov angle for each hit and for each track assuming all photons are originating from the mid point of the track in the radiator. (If the radiator is photon absorbing, move the emission point accordingly.)

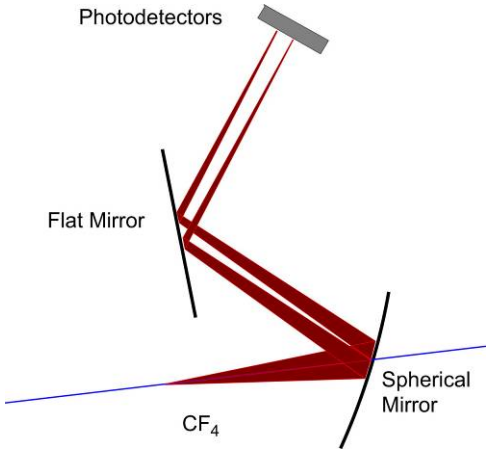

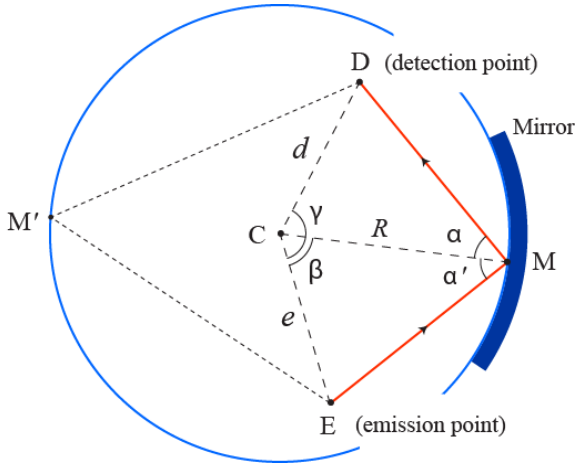

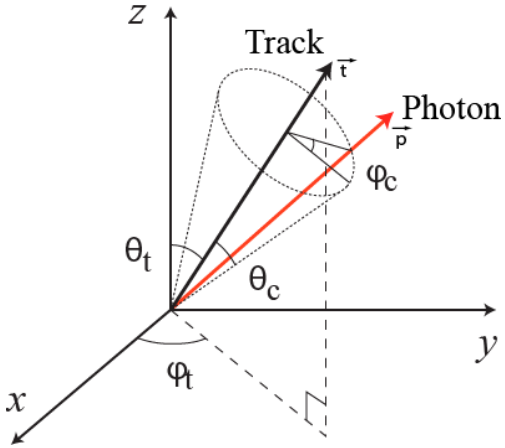

This gives a quartic polynomial in *sin* β which is solved via a resolvent cubic equation.

And then:

$$\cos\Theta_C = \vec{p}\cdot\vec{t}$$

$$\cos\phi_C = \frac{\cos\Theta_t\cos\Theta_C - \cos\Theta_p}{\sin\Theta_t\sin\Theta_C}$$

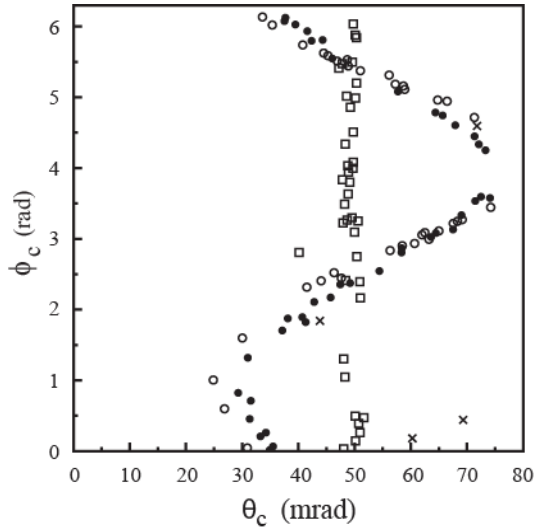

Building the Likelihood.

M^{tot}: Total number of pixels
n_i: number of hits in pixel i
N^{track}: number of tracks to consider
N^{back}: number of background sources to consider
$h=(h_1,h_2, ...,h_N)$ is the event hypothesis. $N=N^{track}+N^{back}$ and h_j: mass hypothesis for track j
$a_{ij}(h_j)$: expected number of hits in pixel i from source j under hypothesis h_j
then the expected signal in pixel i is given by:

$$\nu_i\left(\vec{h}\right)=\sum_{j=1}^{N} a_{ij}\left(h_j\right) \Rightarrow \mathcal{L}\left(\vec{h}\right)=\prod_{i=1}^{M^{tot}} \mathcal{P}_{\nu_i\left(\vec{h}\right)}\left(n_i\right)$$

$$\text{for } \mathcal{P}_{\nu_i\left(\vec{h}\right)}\left(n_i\right)=\frac{e^{-\nu_i\left(\vec{h}\right)}\nu_i\left(\vec{h}\right)^{n_i}}{n_i!} = \text{probability for signal } n_i \text{ when } \nu_i\left(\vec{h}\right) \text{is expected}$$

or

$$\ln \mathcal{L}\left(\vec{h}\right)=-\sum_{j=1}^{N}\mu_j\left(h_j\right)+\sum_{i=1}^{M} n_i \ln \sum_{j=1}^{N} a_{ij}\left(h_j\right)-C$$

$$\text{for } \mu_j\left(h_j\right)=\sum_{i=1}^{M^{tot}} a_{ij}\left(h_j\right) \text{ total expectation from source } j \text{ with } h_j$$

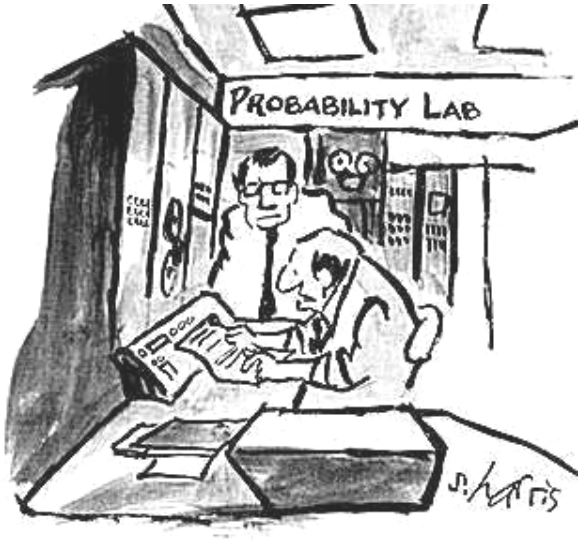

"According to this theory, it's strongly improbable that anything should ever happen anytime, anywhere."

$a_{ij}(h_j)$: the expected number of hits in pixel i from source j under hypothesis h_j
is a function of the detector efficiency ε_i and the expected number of Cherenkov photons arriving at pixel i and emitted by track j under the mass hypothesis h_j.
Let $\lambda_j(h_j)$ be the expected number of Cherenkov photons emitted by track j under the mass hyphenise h_j.
Then

$$a_{ij}(h_j) = \varepsilon_i b_{ij}(h_j) = \varepsilon_i \lambda_j(h_j) \iint_{\text{pixel } i} f_{h_j}(\theta,\phi)\, d\theta d\phi$$

$$\cong \varepsilon_i \lambda_j(h_j) f_{h_j}(\theta_{ij},\phi_{ij}) \iint_{\text{pixel } i} d\theta d\phi$$

$$\approx \varepsilon_i \lambda_j(h_j) f_{h_j}(\theta_{ij},\phi_{ij}) \frac{4A}{R^2\theta_{ij}}$$

Where θ_{ij} and ϕ_{ij} are the reconstructed angles.

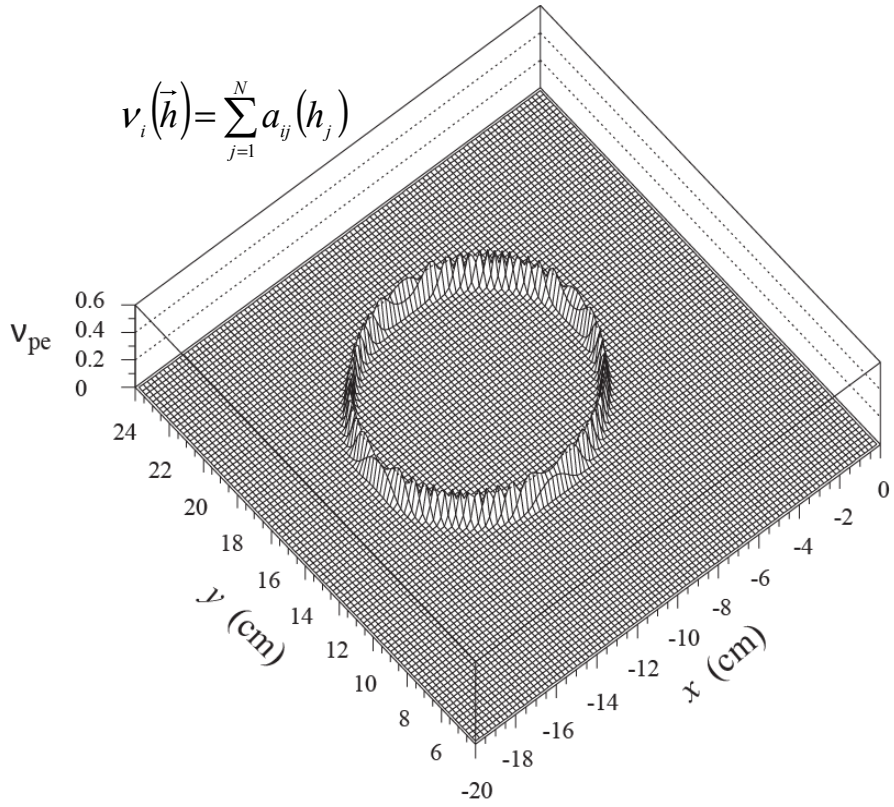

Expected number of photoelectrons in each pixel

Then add:

- Photon scattering like Rayleigh and Mie
- Mirror inaccuracy
- Chromatic aberration
- .....

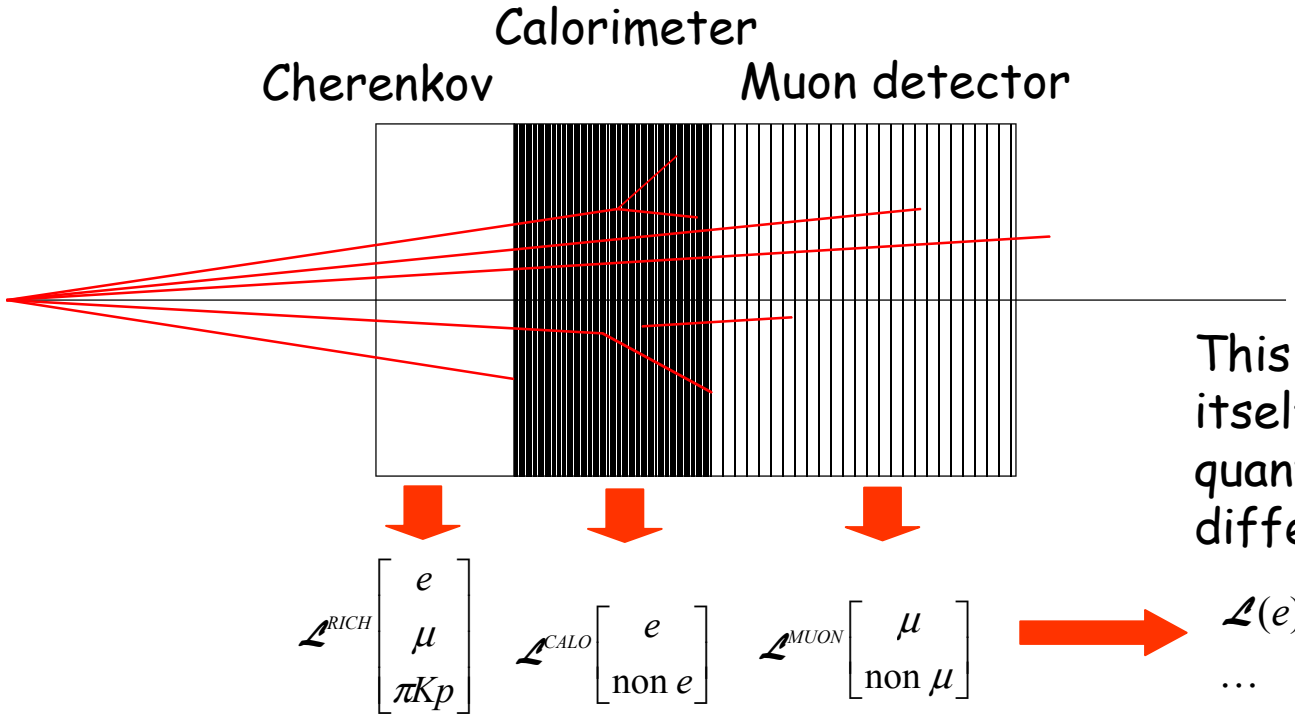

This absolute likelihood value itself is not the useful quantity since the scale will be different for each event.

$$\mathcal{L}(e) = \mathcal{L}^{RICH}(e) \cdot \mathcal{L}^{CALO}(e) \cdot \mathcal{L}^{MUON}(\text{non } \mu)$$
$$\ldots$$

Rather use the differences in the log-likelihoods:

$$\Delta \ln \mathcal{L}_{K\pi} = \ln \mathcal{L}(K) - \ln \mathcal{L}(\pi)$$

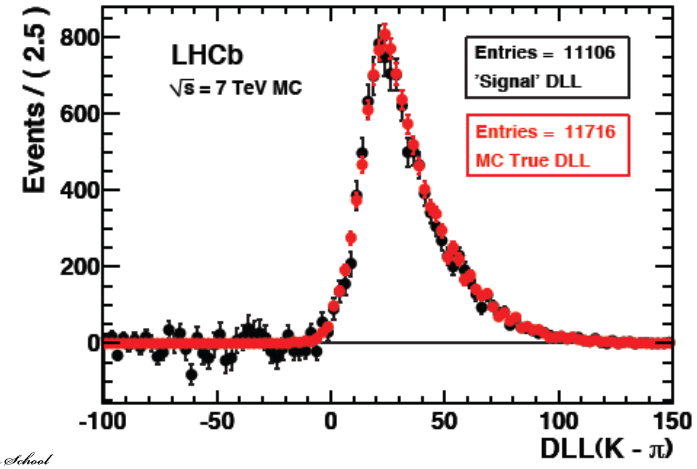

$\Delta \log \mathcal{L}(\mathrm{K} - \pi)$

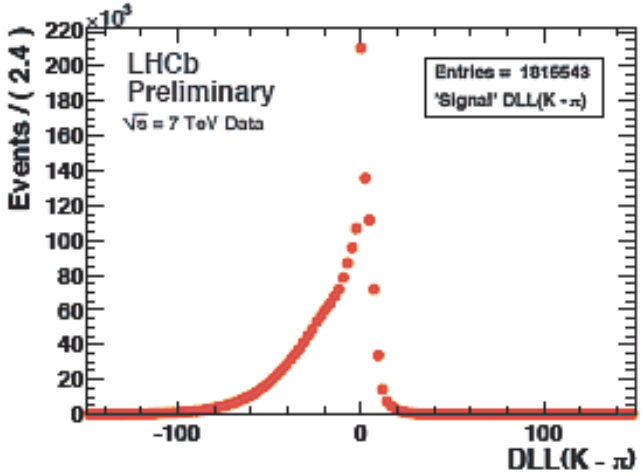

LHCb preliminary

pbar/p analysis

DLL in p-K, p-π space for pions, kaons and protons (obtained from data calibration samples) in one bin in p_t,η space.
Top right box is region selected by cuts.

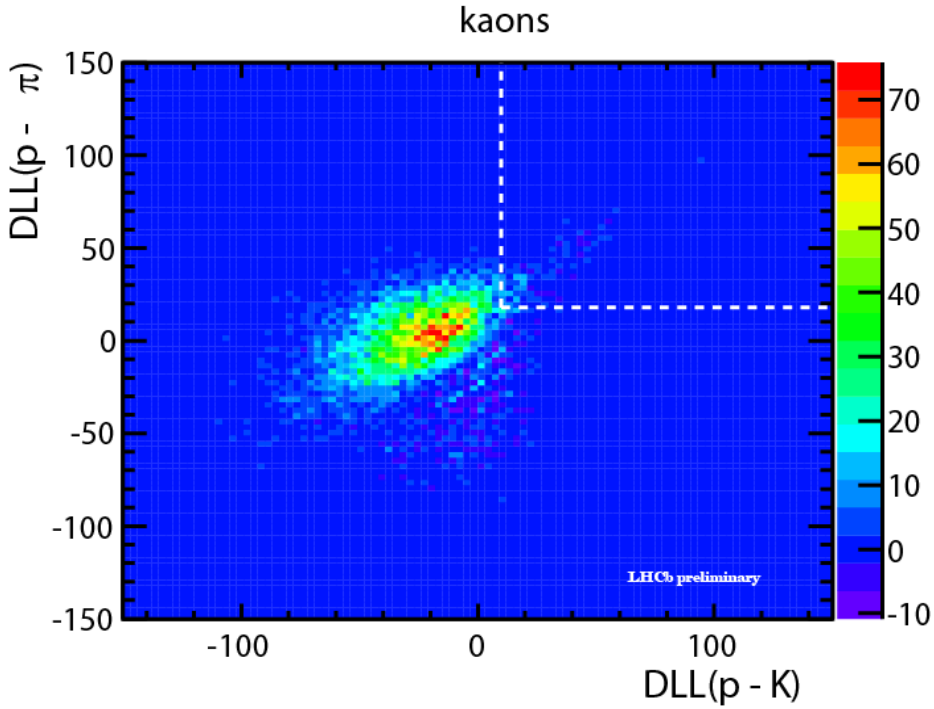

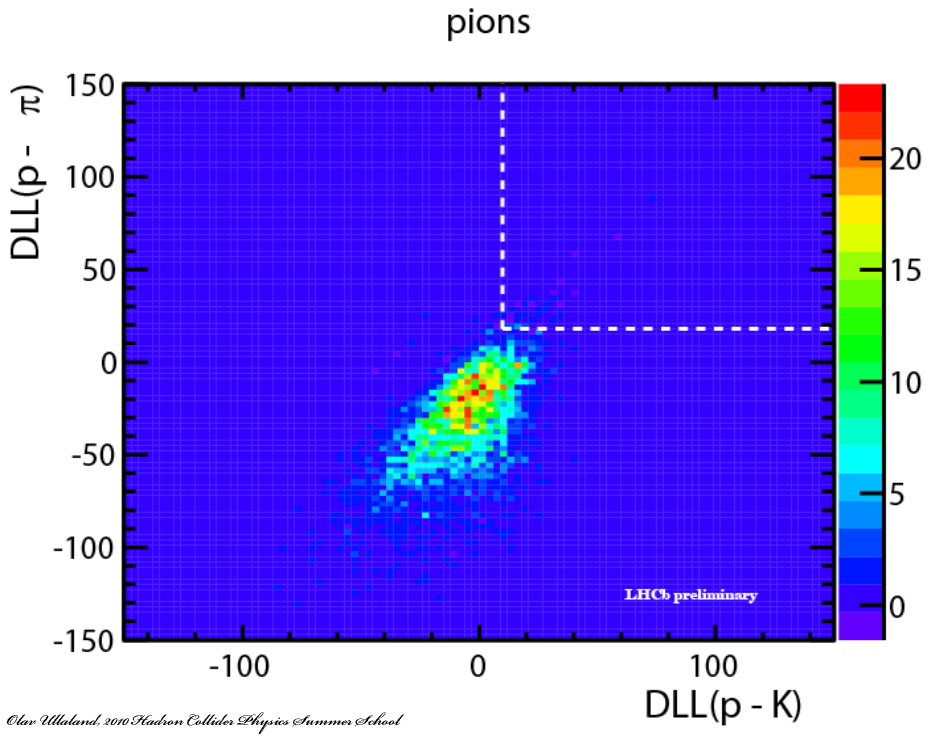

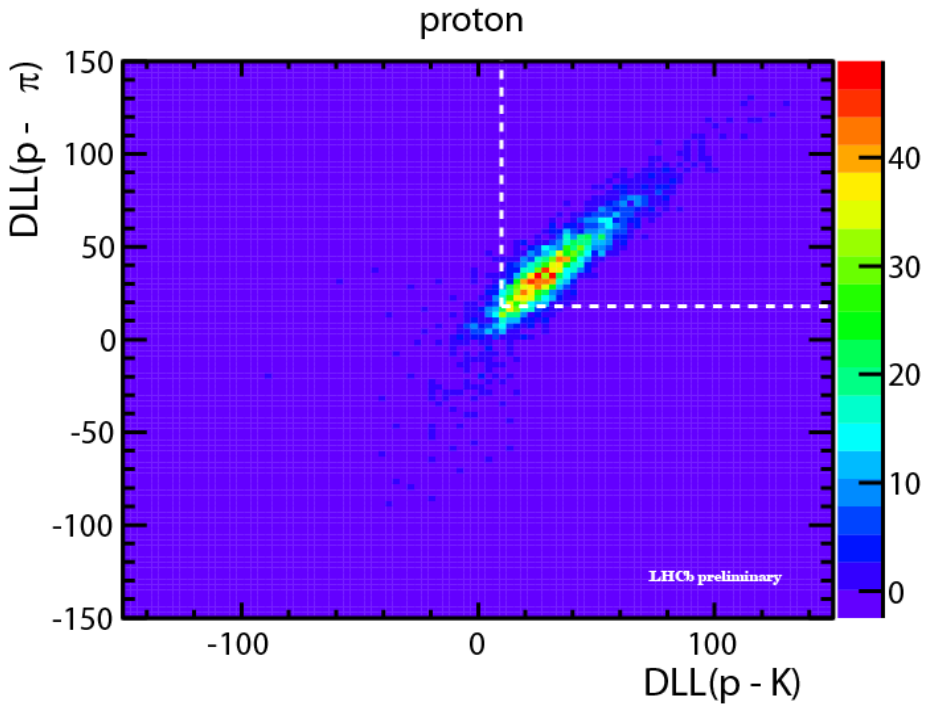

It is not sufficient to confirm the efficiency. Misidentification must also be assessed.

Plots demonstrating the LHCb RICH performance from assessment of a Monte Carlo $D^{*\pm}$ selection sample.
The efficiency to correctly identify
(a) pions
and
(b) kaons
as a function of momentum is shown by the **red data points**.

The corresponding misidentification probability is shown by the **blue data points**. The events selected to generate both plots possessed high quality long tracks

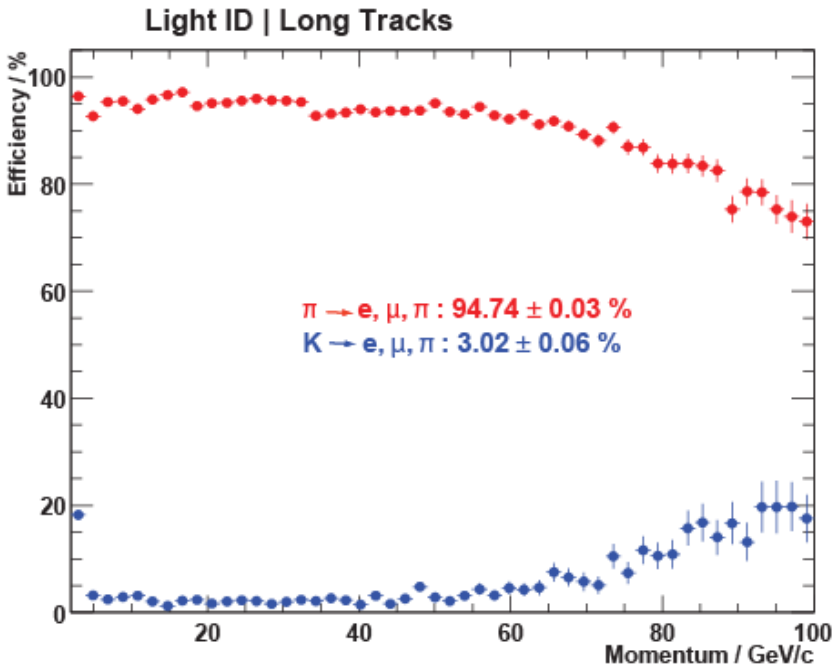

(a)

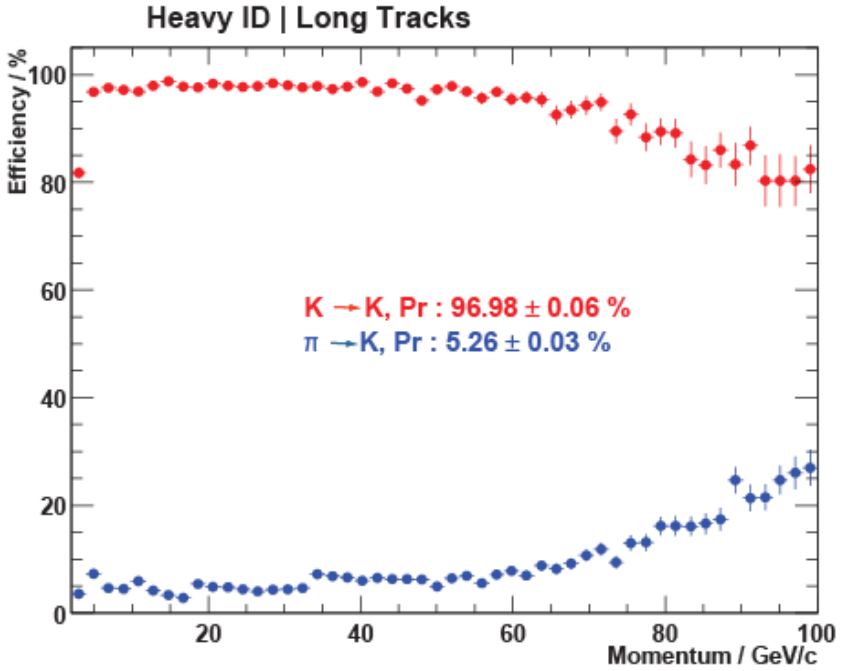

(b)

A. Powell, CERN-THESIS-2010-010 - Oxford : University of Oxford, 2009.

Trackless ring finding

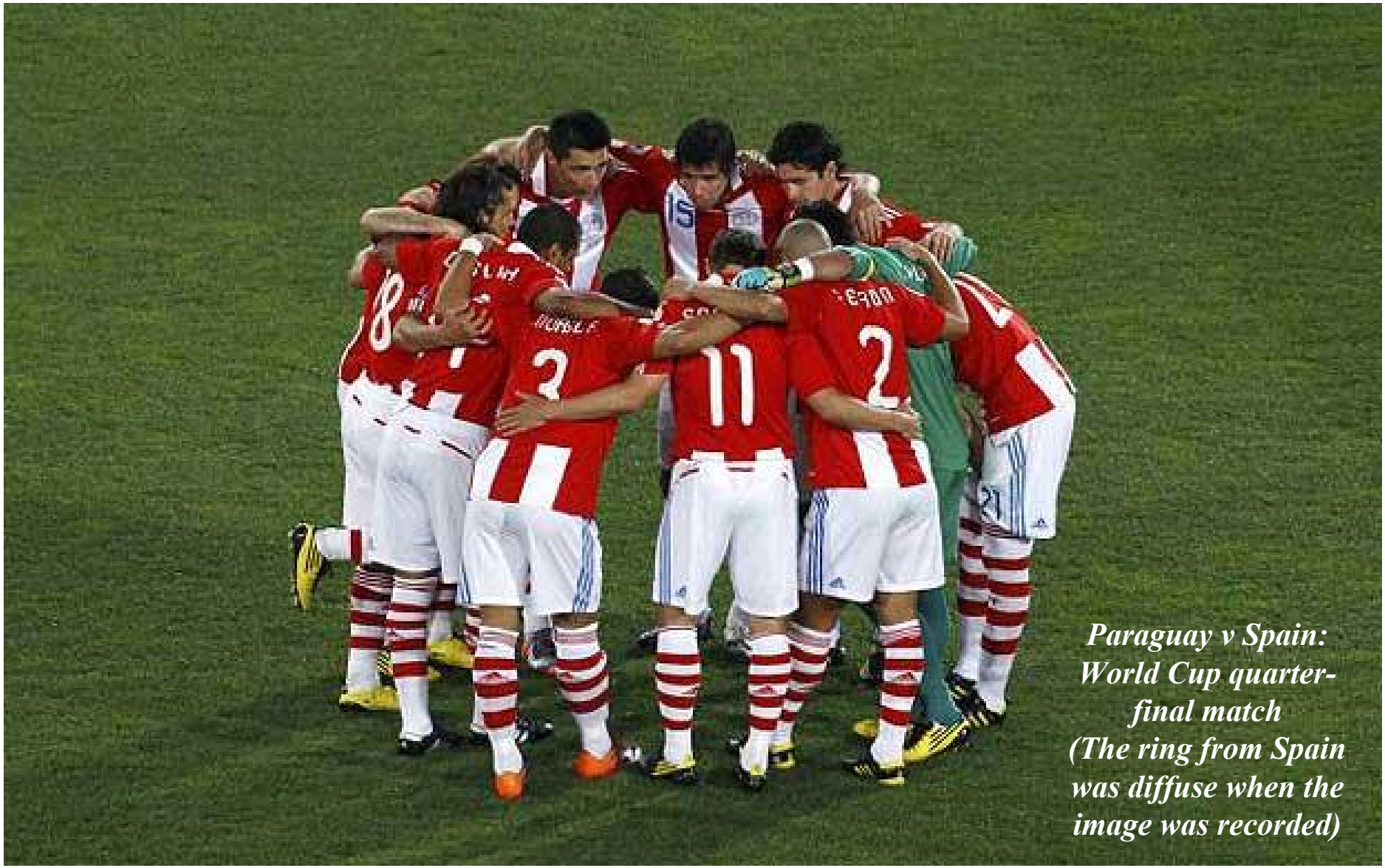

Paraguay v Spain: World Cup quarter-final match (The ring from Spain was diffuse when the image was recorded)

Trackless Ring Reconstruction

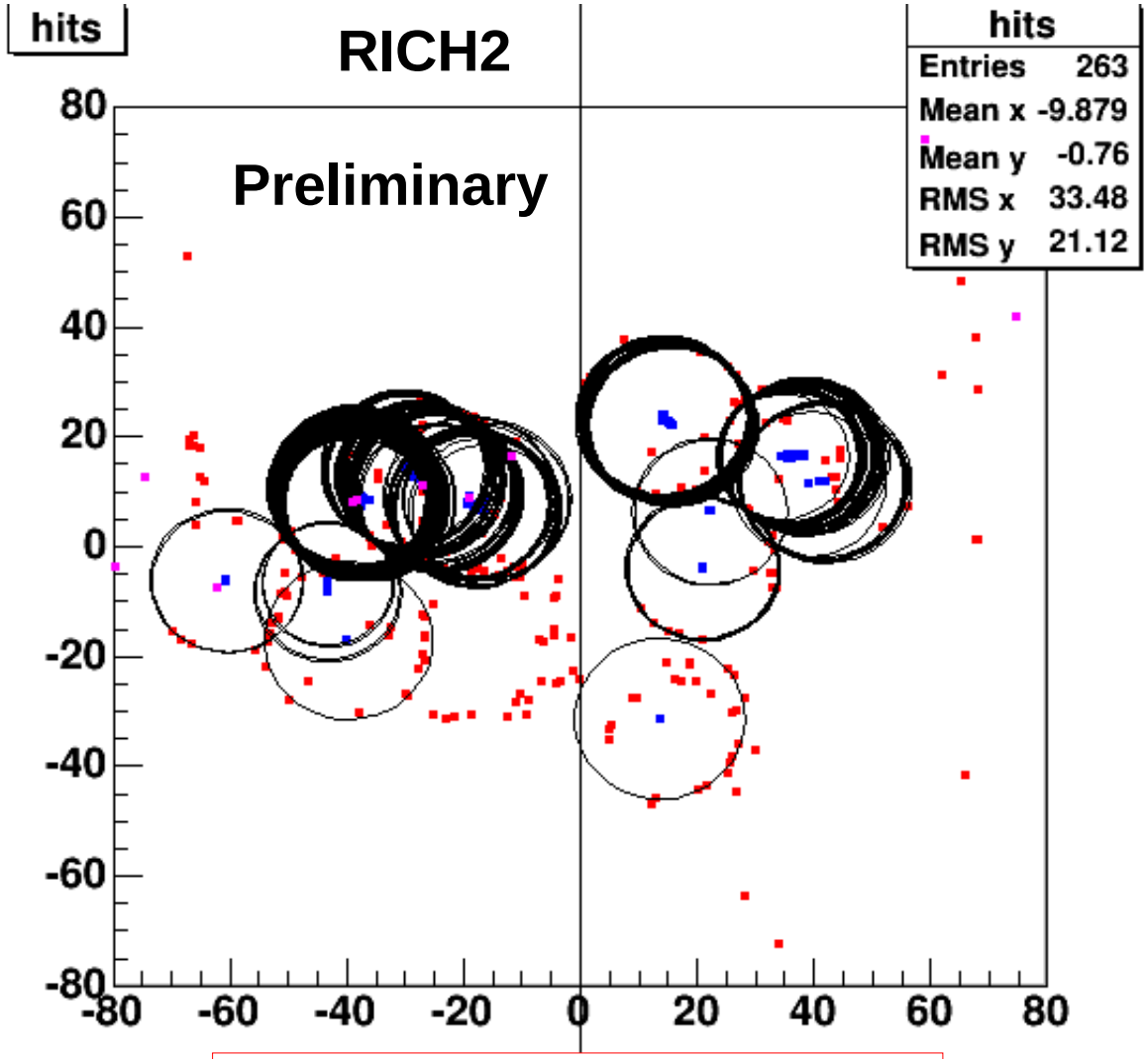

hits, Hough centres, track impact points

Hough transform:

Reconstruct a given family of shapes from discrete data points, assuming all the members of the family can be described by the same kind of equation. To find the best fitting members of the family of shapes the image space (data points) is mapped back to parameter space.

from Cristina Lazzeroni, Raluca Muresan, CHEP06

Trackless Ring Reconstruction_____2

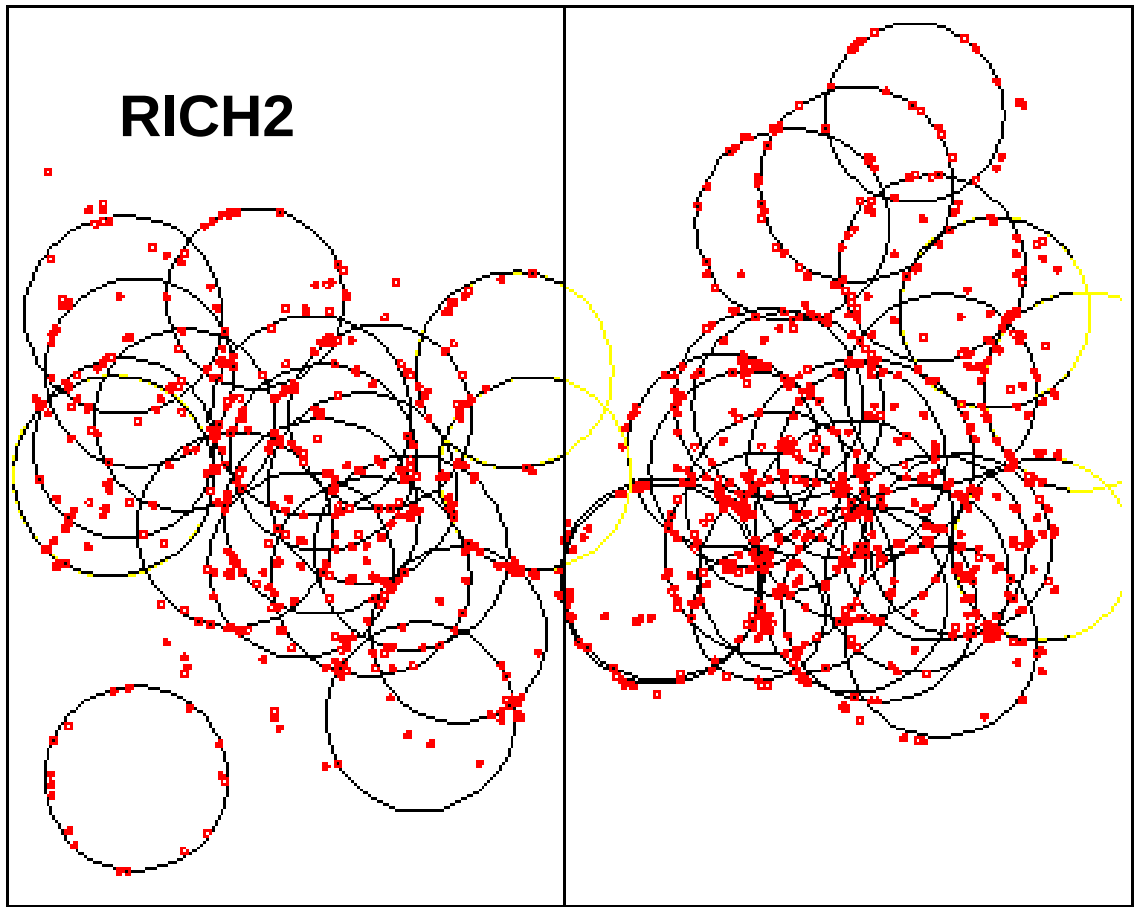

Markov rings

Metropolis- Hastings Markov chains:

Sample possible ring distributions according to how likely they would appear to have been given the observed data points. The best proposed distribution is kept.

(Preliminary results are encouraging, work on going to assess the performance of the method)

from Cristina Lazzeroni, Raluca Muresan, CHEP06

Some ways to work with quartz.

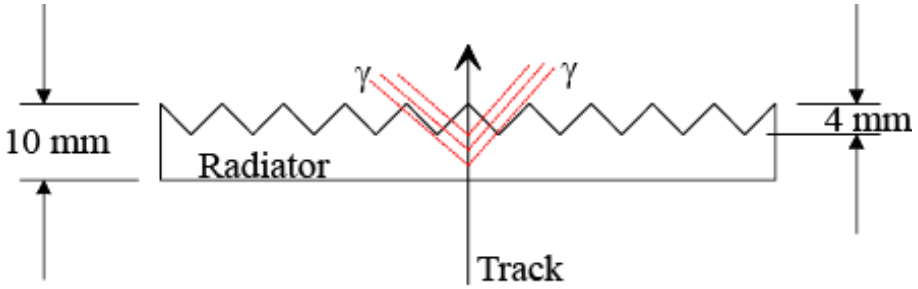

http://www.lepp.cornell.edu/Research/EPP/CLEO/
Nucl. Instr. and Meth. in Phys. Res. A 371(1996)79-81
CLEO at Cornell electron storage rings.

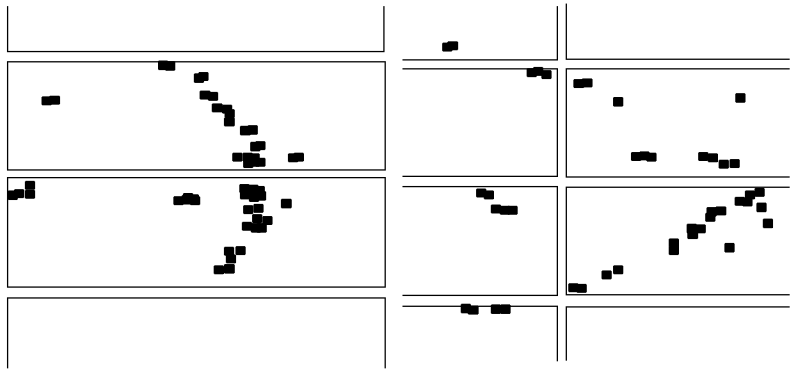

Hit patterns produced by the particle passing the plane (left) and saw tooth (right) radiators

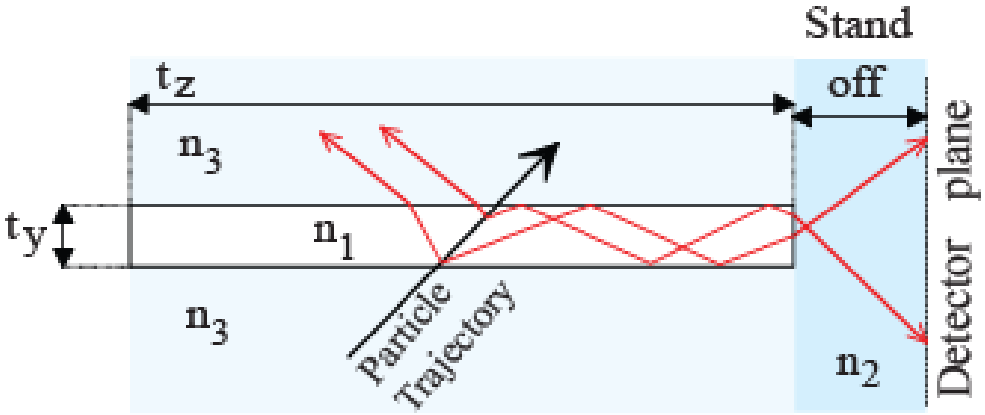

Schematic of the radiator bar for a DIRC detector.
Nucl. Instr. and Meth. in Phys. Res. A 343(1994)292-299
http://www.slac.stanford.edu/BFROOT/www/Detector/DIRC/PID.htm

The standoff region is designed to maximize the transfer efficiency between the radiator and the detector.
If this region has the same index of refraction as the radiator, $n_1 \cong n_2$, the transfer efficiency is maximized and the image will emerge without reflection or refraction at the end surface.

DIRC

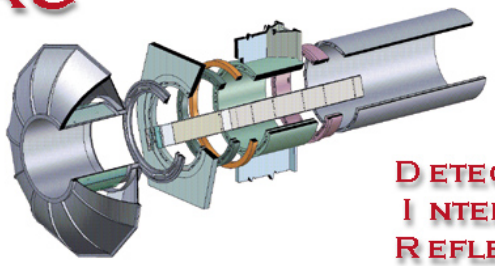

DETECTION OF
I NTERNALLY
R EFLECTED
C HERENKOV LIGHT

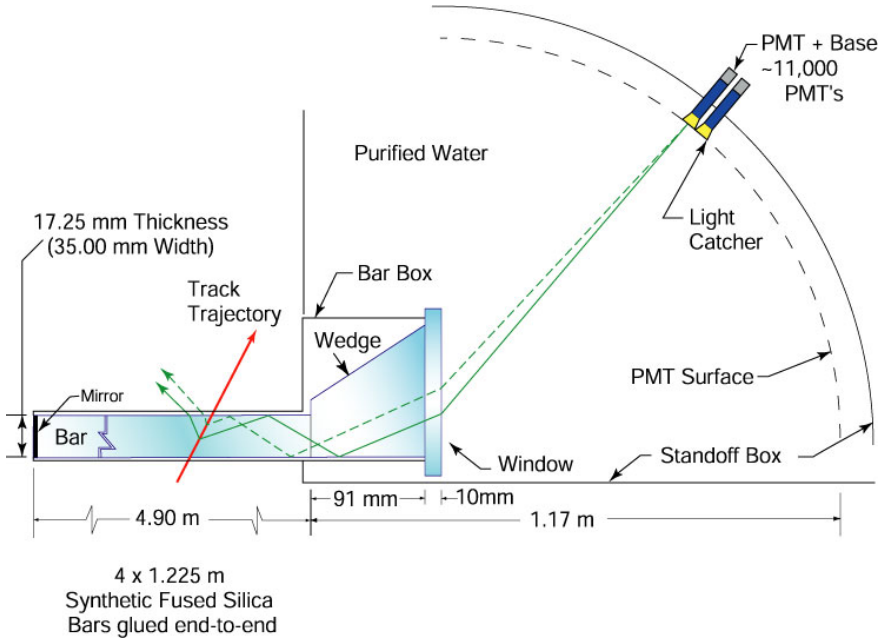

from Jochen Schwiening: RICH2002, Nestor Institute, Pylos, June 2002

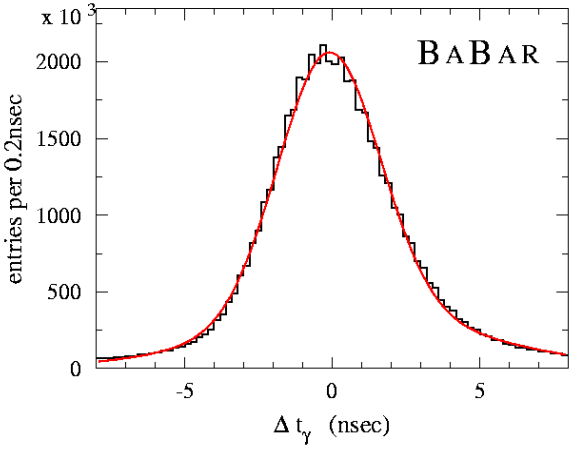

± 300 nsec trigger window
(~500-1300 background hits/event)

→

± 8 nsec Δt window
(1-2 background hits/sector/event)

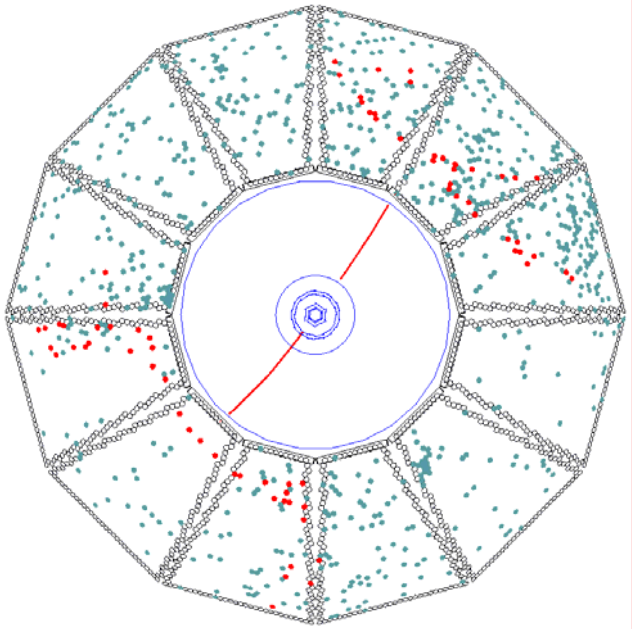

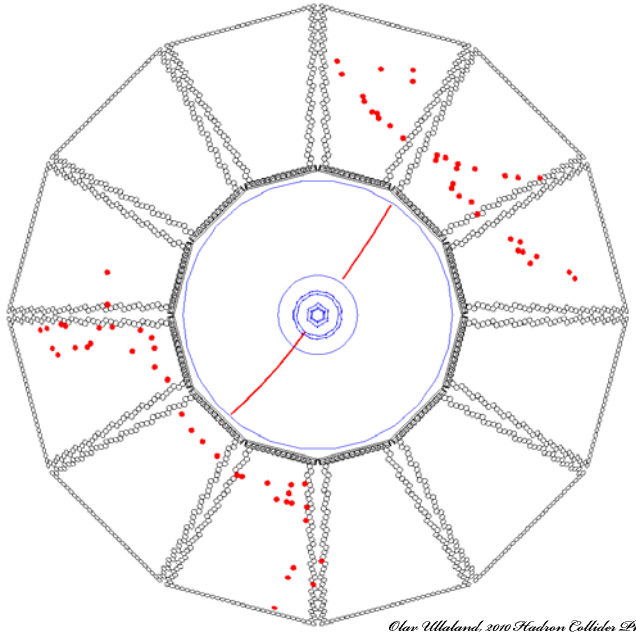

TORCH concept

- I am currently working on the design of a new concept for Particle ID for the upgrade of LHCb (planned to follow after ~ 5 years of data taking)
- Uses a large plate of quartz to produce Cherenkov light, like a DIRC
  But then identify the particles by measuring the photon arrival times
  Combination of **TO**F and **RICH** techniques → named TORCH
- Detected position around edge gives photon angle (θ_x)
  Angle (θ_z) out of plane determined using focusing
  Knowing photon trajectory, the track arrival time can be calculated

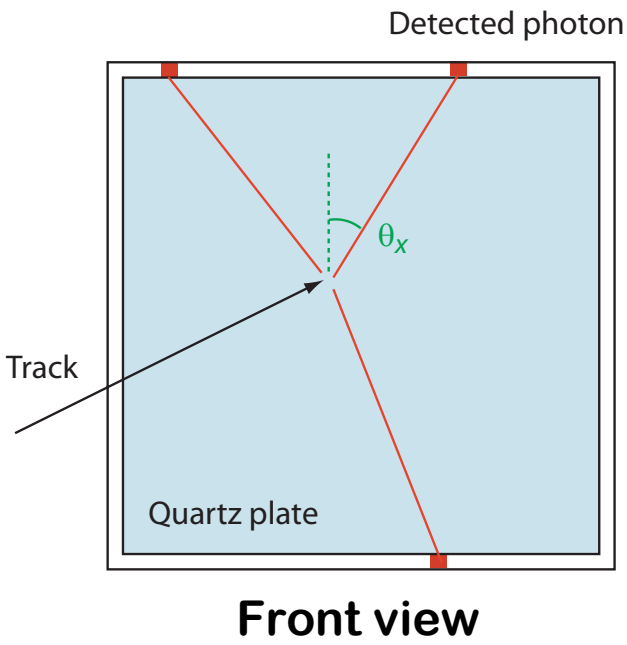

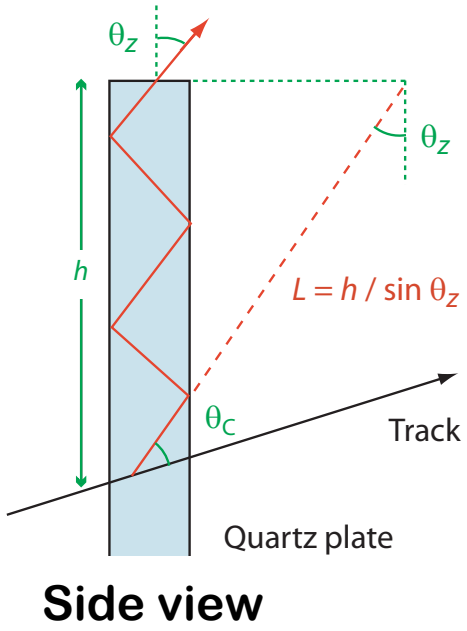

Proposed layout

- Optical element added at edges to focus photons onto MCP detectors
  It converts the angle of the photon into a position on the detector

Schematic layout

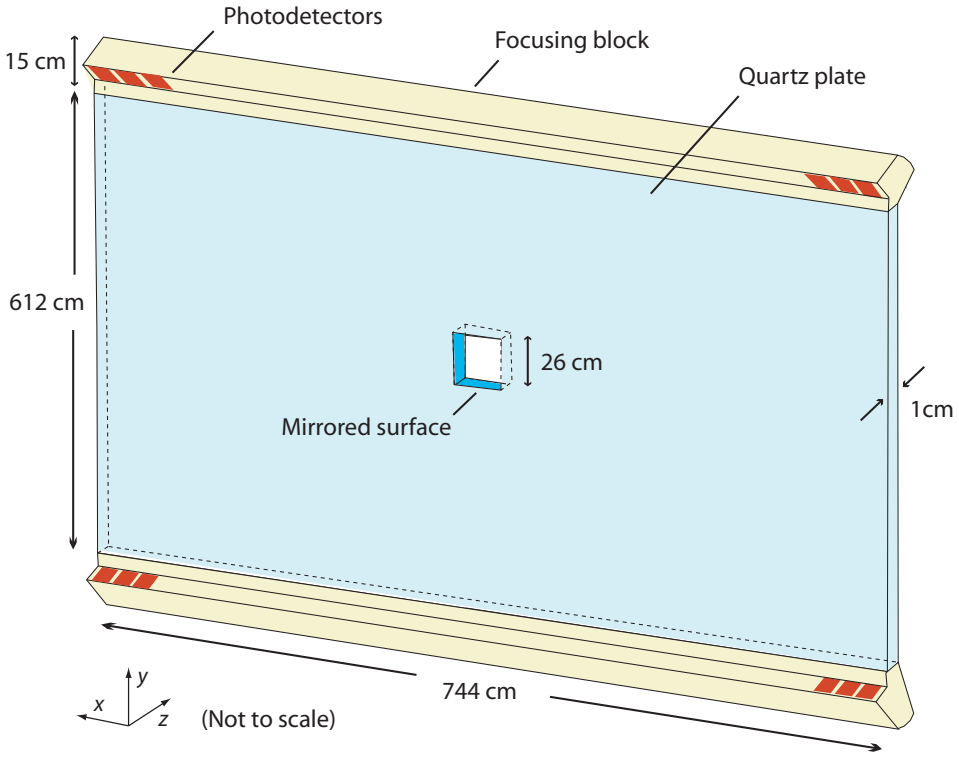

Focusing element

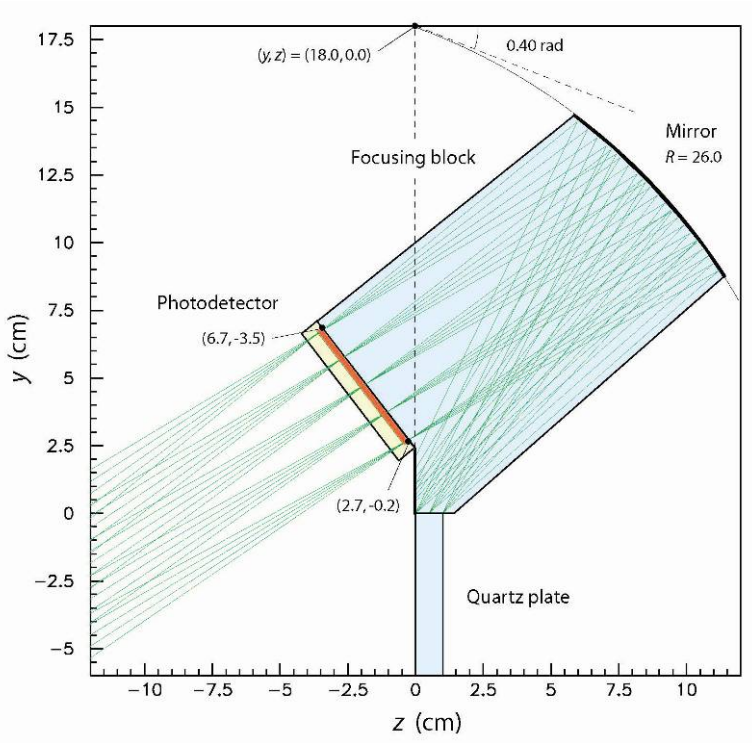

Predicted performance

- Pattern recognition will be a challenge, similar to a DIRC
- Assuming a time resolution per detected photon of 50 ps,
  the simulated performance gives 3σ K-π separation up to > 10 GeV
  Will need to be confirmed with an R&D program using test detectors

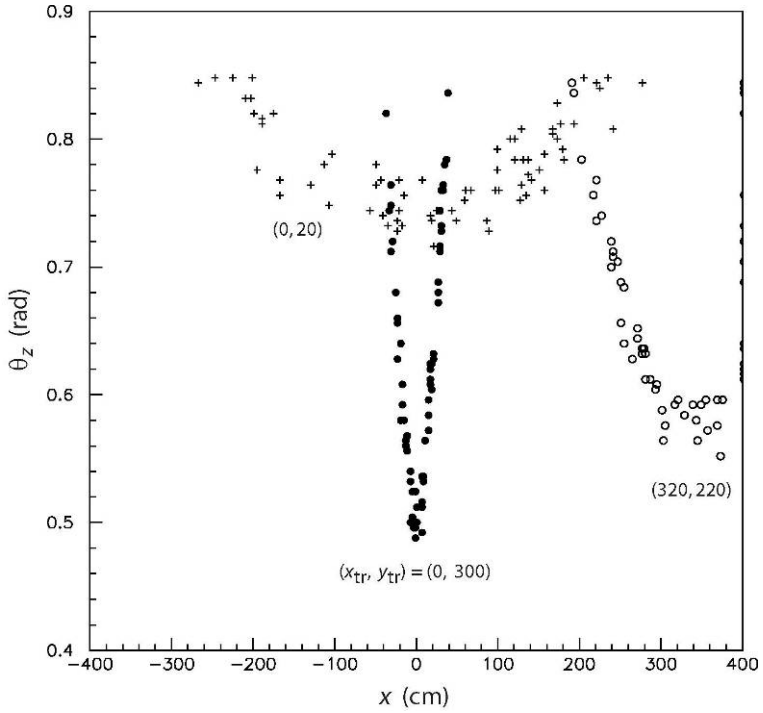

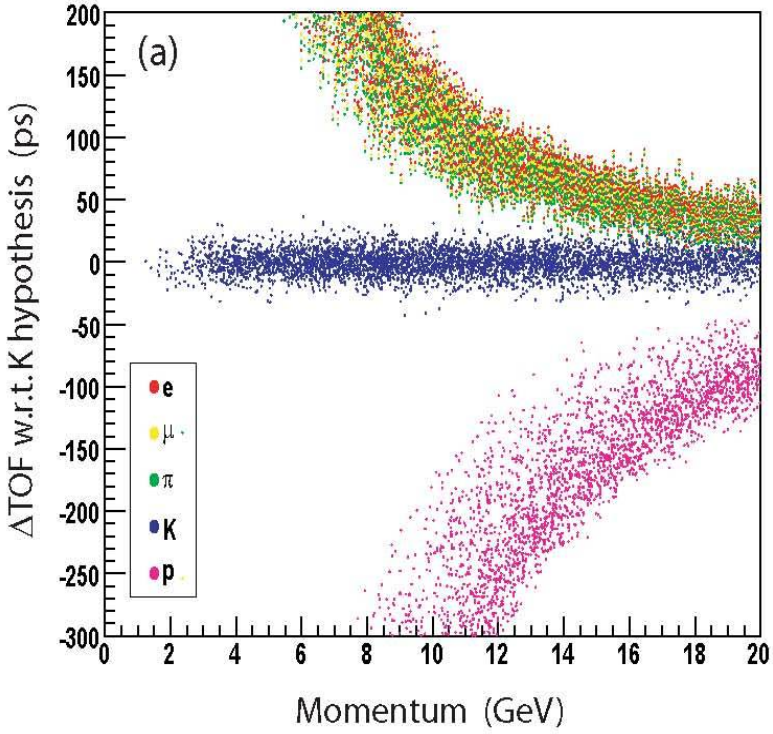

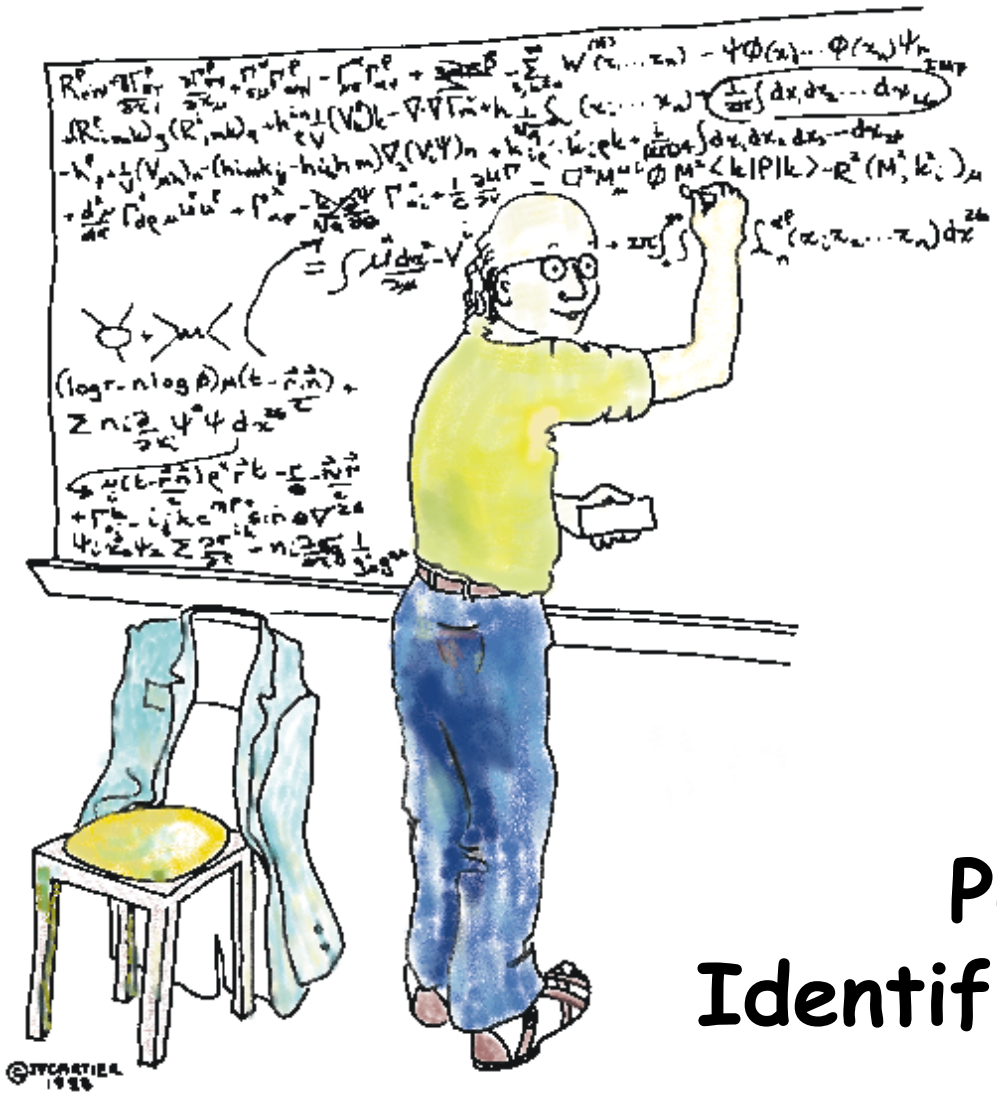

At this point we notice that this equation is beautifully simplified if we assume that particle identification has 92 dimensions and transition radiation can be added as a subset.

Particle Identification with Transition Radiation

Transition Radiation. A primer.

A quote from
M.L.Ter-Mikaelian, High-Energy Electromegnetic Processes in Condensed Media, John Wiley & Sons, Inc, 1972, ISBN 0-471-85190-6 :

We believe that the reader will find it more convenient, however, to derive the proper formulas by himself, instead of perpetuating the particularities of all the original publications. This is due to the fact that the derivation of the corresponding formulas (for oblique incidence and in the case of two interfaces in particular), usually based on well-known methods, requires simple although time-consuming algebraic calculations.

We will not do that.

V.L. Ginzburg and I.M. Frank predicted in 1944 the existence of transition radiation. Although recognized as a milestone in the understanding of quantum mechanics, transition radiation was more of theoretical interest before it became an integral part of particle detection and particle identification.

Start a little slow with Transition Radiation.

Schematic representation of the production of transition radiation at a boundary.

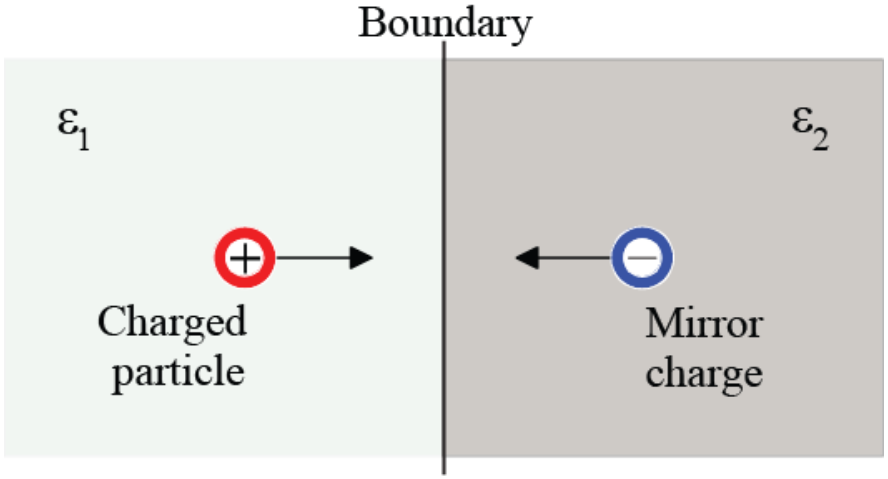

Transition radiation as function of the emission angle for $\gamma = 10^3$

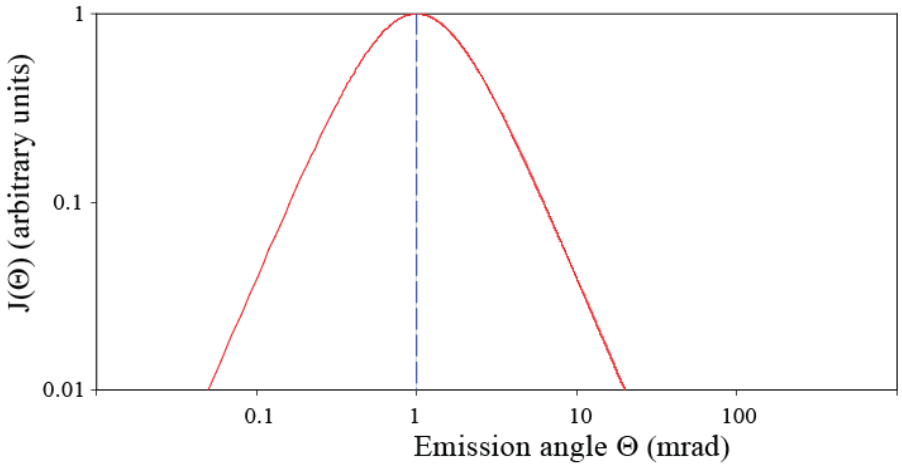

For a perfectly reflecting metallic surface:

$$J(\Theta) = \omega \frac{dN}{d\omega d\Omega} = \frac{\alpha}{\pi^2}\left(\frac{\Theta}{\gamma^{-2} + \Theta^2}\right)^2$$

Energy radiated from a single surface:

$$\varepsilon_0 \rightarrow \varepsilon$$

$$W = \frac{1}{3}\alpha Z^2 \omega_p \gamma$$

ω_p : plasma frequency

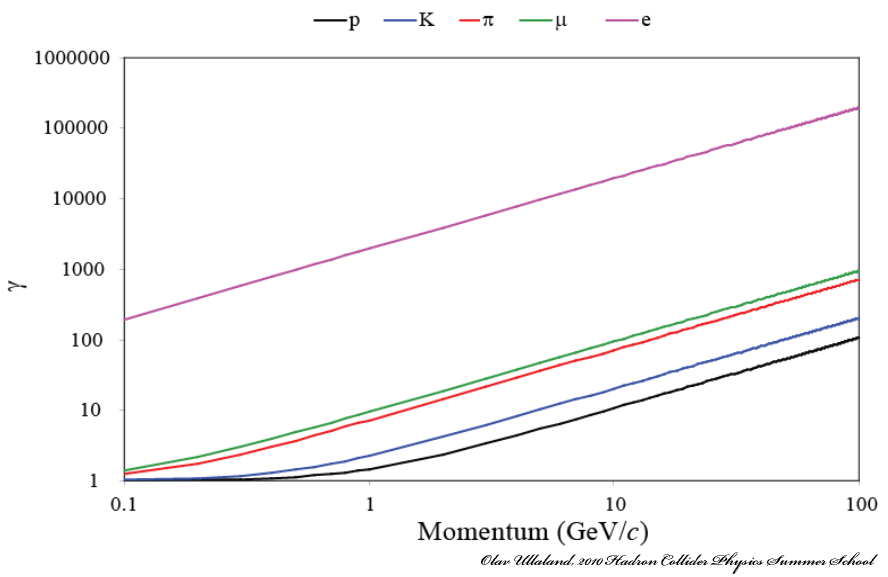

Formation zone.

The transient field has a certain extension:

$$\text{Formation zone}: d = \frac{2c}{\omega}\left[\gamma^{-2} + \Theta^2 + \left(\frac{\omega_p}{\omega}\right)^2\right]$$

$$\text{for } \Theta = \gamma^{-1} \text{ or } \omega = \frac{1}{\sqrt{2}}\gamma\omega_p$$

$$d(\mu\text{m}) \approx 140 \cdot 10^{-3} \frac{\gamma}{\omega_p(\text{eV})}$$

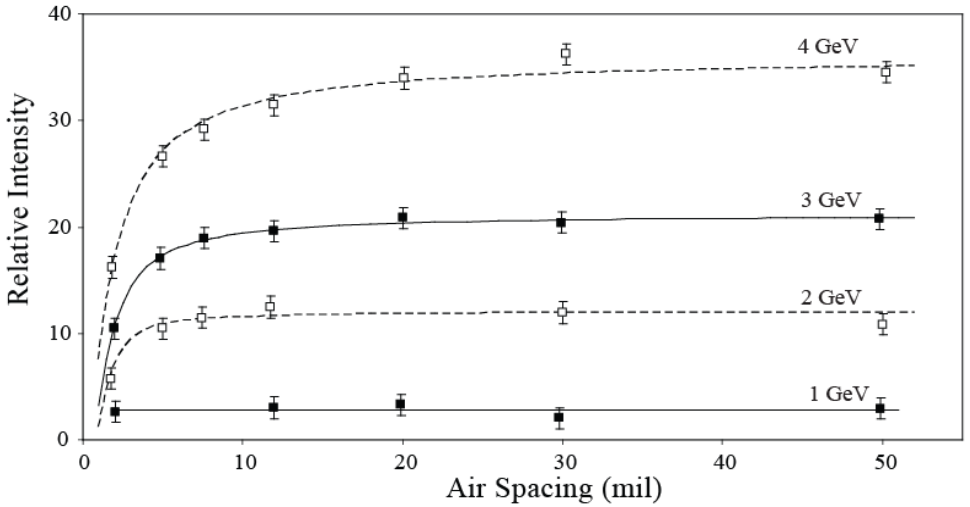

Relative intensity of transition radiation for different air spacing. Each radiator is made of 231 aluminium foils 1 mil thick. (1 mil = 25.4 μm). Particles used are positrons of 1 to 4GeV energy (γ = 2000 to 8000). Phys. Rev. Lett. 25 (1970) 1513-1515

1. Transition radiation is **a prompt signal**.
2. Transition radiation is **not a threshold phenomenon**.
3. The total radiated power from a single interface **is proportional to γ**.
4. The mean emission angle is **inversely proportional to γ**.

I will only cover detectors working in the X-ray range.

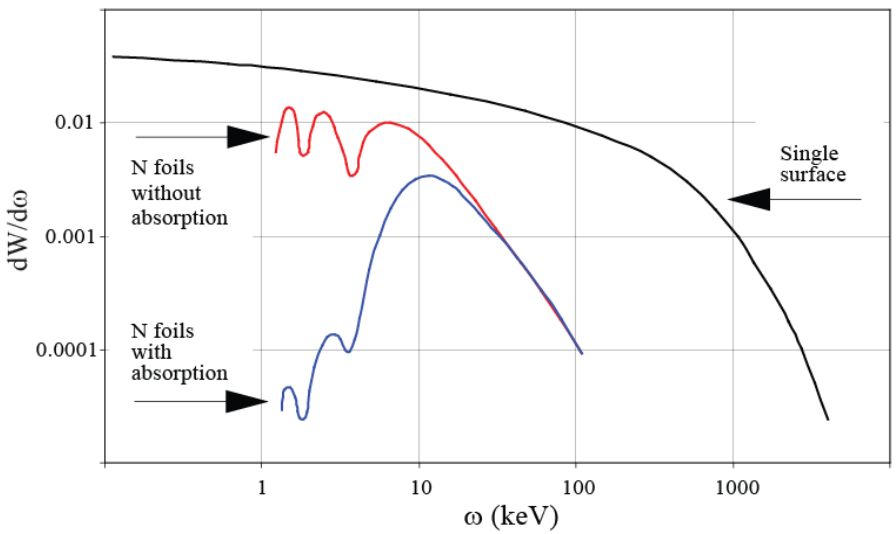

Intensity of the forward radiation divided by the number of interfaces for 20 μm polypropylene (ω_p = 21 eV) and 180 μm helium (ω_p = 0.27 eV).
L. Fayard, Transition radiation, les editions de physiques, 1988, 327-340

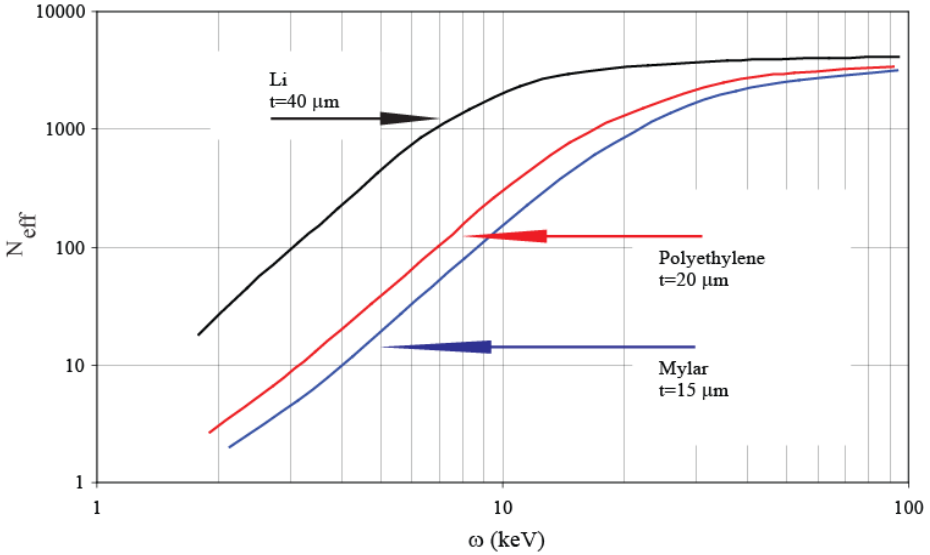

The effective number of foils in a radiator as function of photon energy.
Nucl. Instrum. Methods Phys. Res., A: 326(1993) 434-469

An efficient transition radiation detector is therefore a large assembly of radiators interspaced with many detector elements optimised to detect X-rays in the 10 keV range.

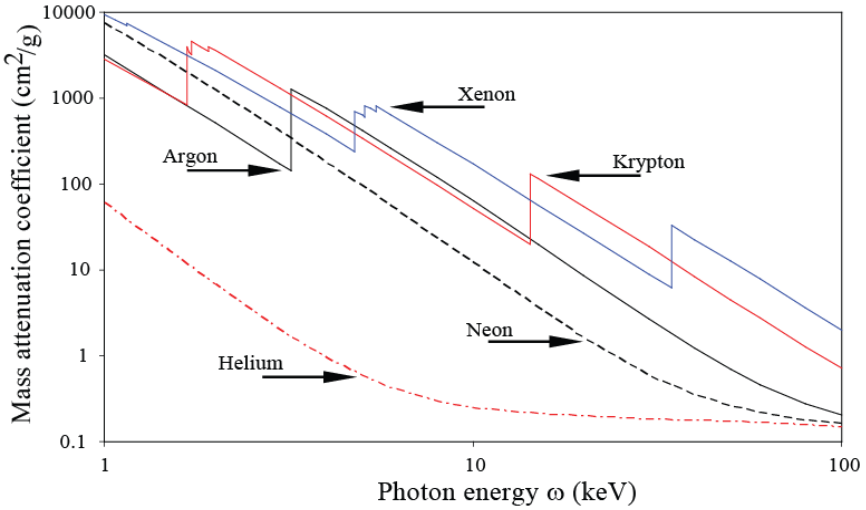

X-ray mass attenuation coefficient, μ/ρ, as function of the photon energy. $\mu/\rho = \sigma_{tot}/uA$, where $u = 1.660 \times 10^{-24}$ g is the atomic mass unit, A is the relative atomic mass of the target element and σ_{tot} is the total cross section for an interaction by the photon.

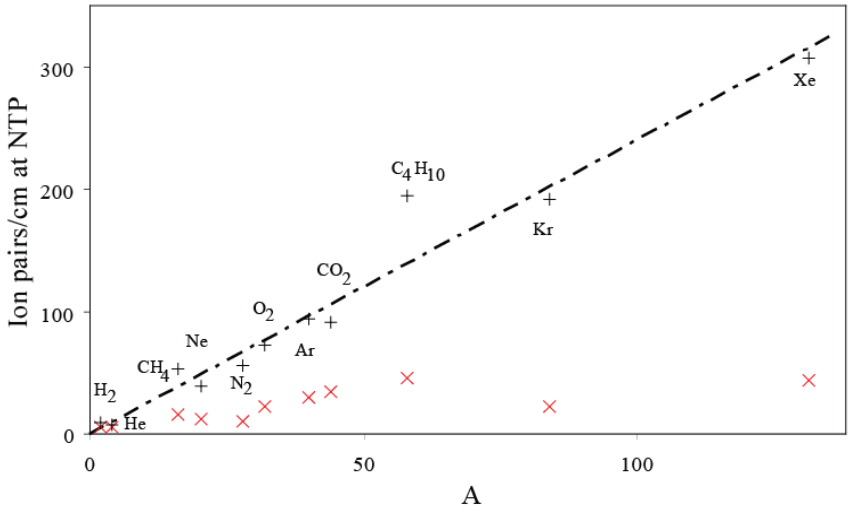

The (×) primary and (+) total number of ion pairs created for a minimum ionizing particle per cm gas at normal temperature and pressure as function of A.

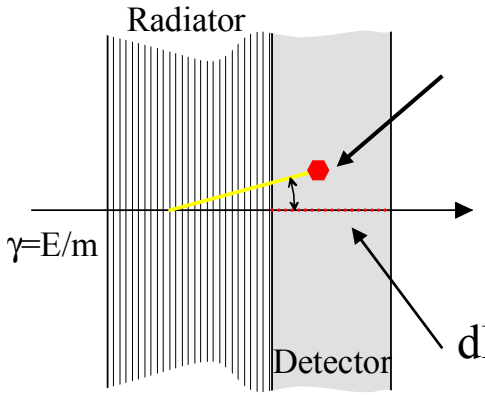

Not to scale

10-15 mm Xe

~22 eV/ion pair. 10 keV X-ray → ~450 ion pairs

dE/dX_{MIP}~310 ion pairs/cm * relativistic rise ~550 ion pairs/cm

Additional background might arise from curling in a magnetic field, Bremsstrahlung and particle conversions.

Use ATLAS as an example. http://atlas.web.cern.ch/Atlas/Collaboration/

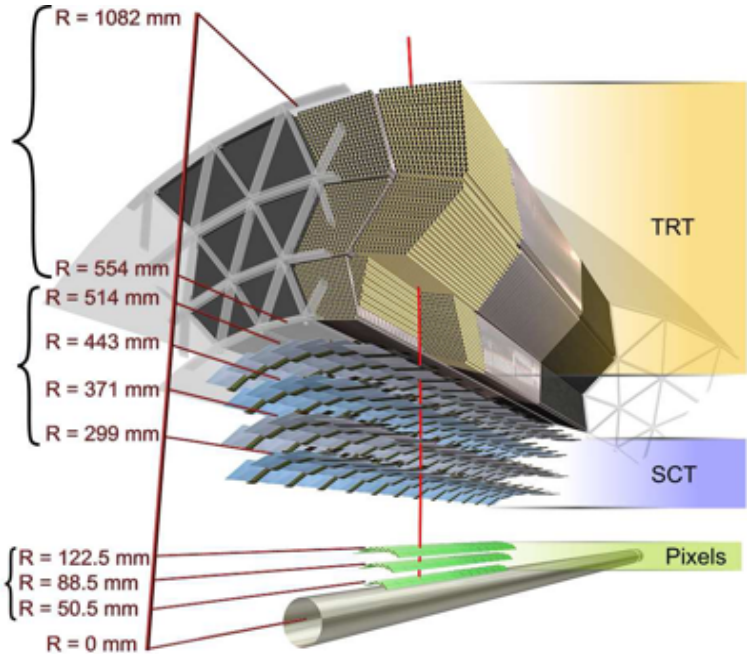

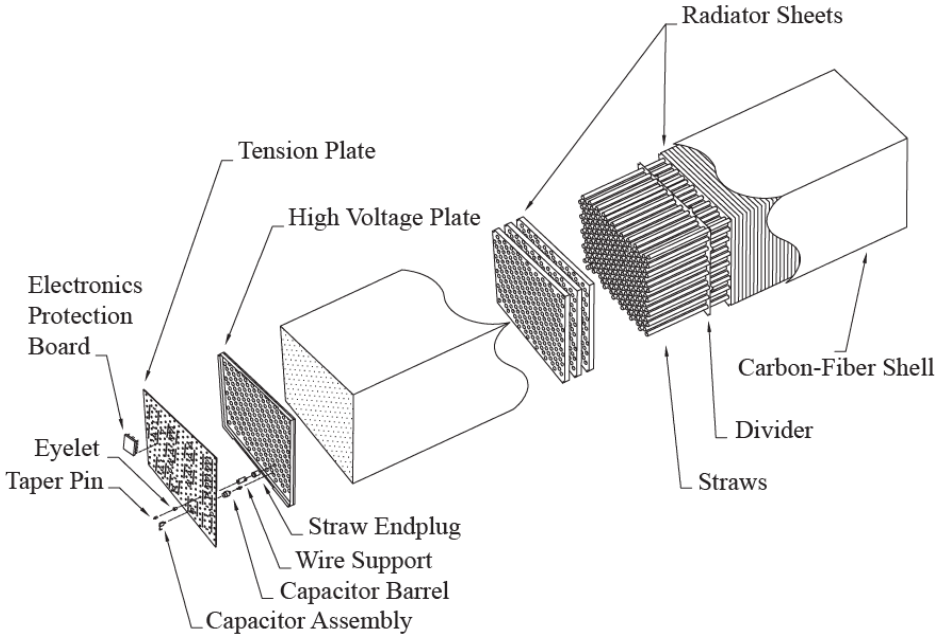

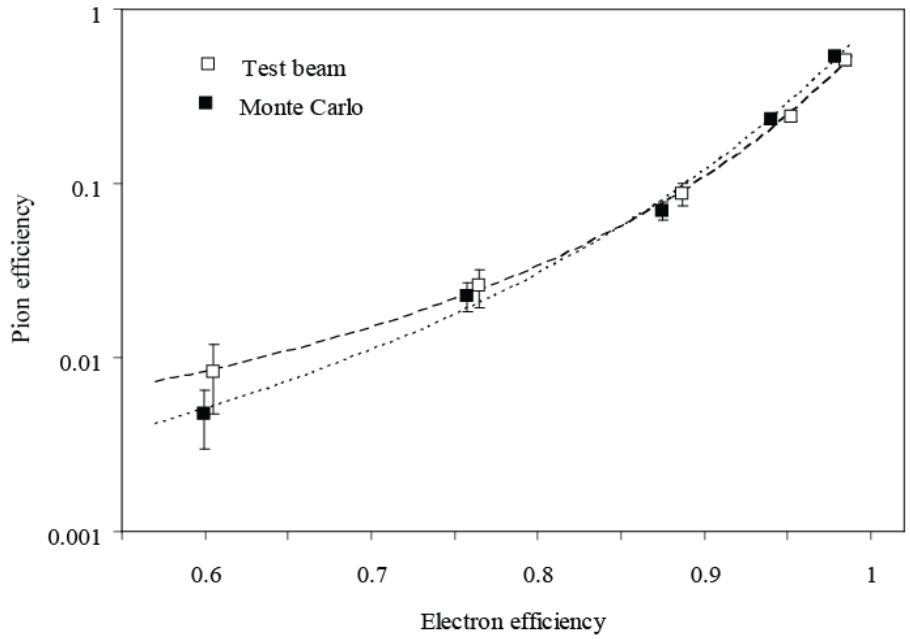

Normalized Time-over-Threshold in TRT

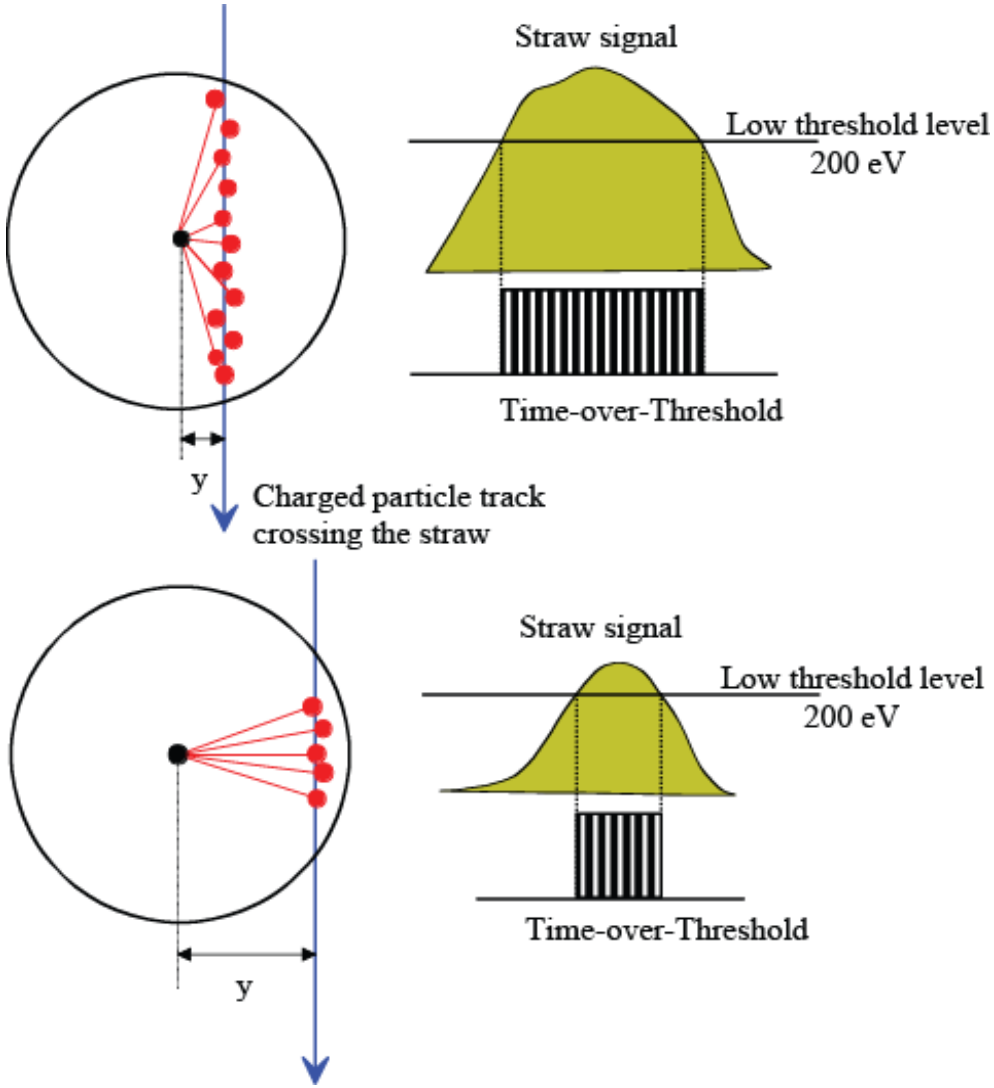

Time-over threshold depends on

- Energy deposited through ionization loss
- Depends on particle type
- Length of particle trajectory in the drift tube

- Study uses only low-threshold hits to avoid correlation with PID from high-threshold hit probability

from Kerstin Tackmann (CERN) ATLAS Inner Detector Material Studies, June 7, 2010 – Hamburg, Germany

Electron PID from the TRT

- Transition radiation (depending on Lorentz γ) in scintillating foil and fibres generate high threshold hits in TRT
- Turn-on for $e^{\pm}$ around $p > 2$ GeV
- Photon conversions supply a clean sample of $e^{\pm}$ for measuring HT probability at large γ
  - Tag-and-probe: Select good photon conversions, but require large HT fraction only on one leg
- $\pi^{\pm}$ sample for calibration at small γ
  - Require B-layer hit
  - Veto tracks overlapping with conversion candidates

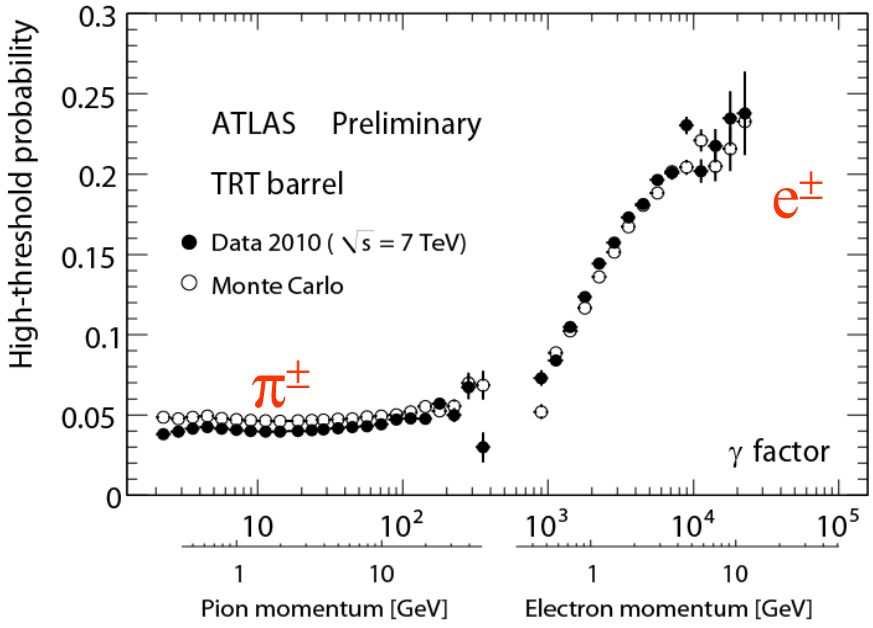

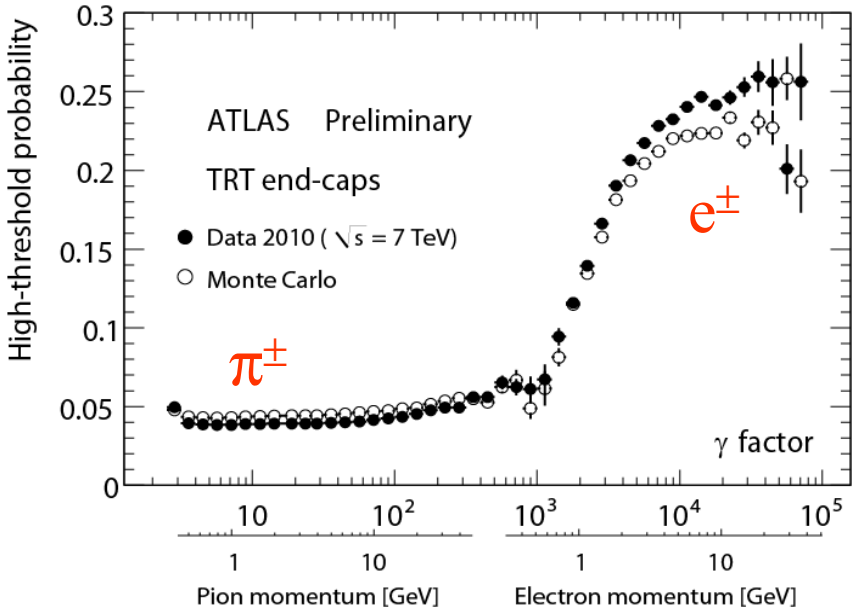

from Kerstin Tackmann (CERN) ATLAS Inner Detector Material Studies, June 7, 2010 – Hamburg, Germany
see also https://twiki.cern.ch/twiki/bin/view/Atlas/TRTPublicResults

That was all
planned for this lecture

Spare slides and back-ups

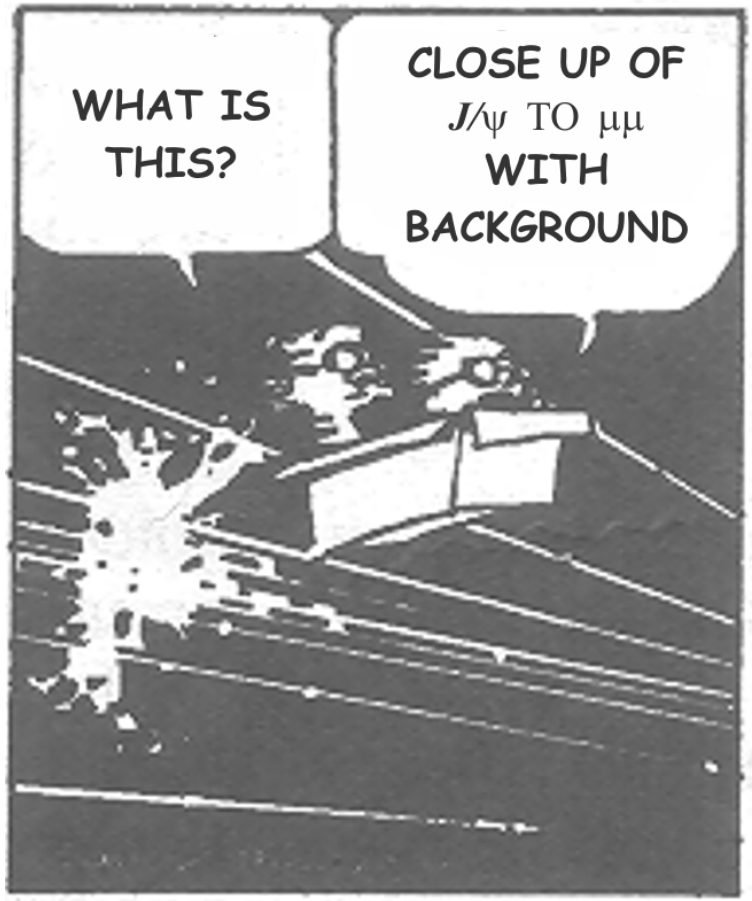

Kolmogorov-Smirnov tests

There is more to it than what is written here! Frodesen et al., probability and statistics in particle physics, 1979

Assume a sample of n uncorrelated measurements x_i. Let the series be ordered such that $x_1<x_2<$ ... Then the cumulative distribution is defined as:

$$S_n(x)=\begin{cases} 0 & x < x_1 \\ i/n & x_i \le x < x_{i+1} \\ 1 & x \ge x_n \end{cases}$$

The theoretical model gives the corresponding distribution $F_0(x)$

The null hypothesis is then H_0: $S_n(x)=F_0(x)$

The statistical test is: $D_n=max|S_n(x)-F_0(x)|$

Example

In 30 events measured proper flight time of the neutral kaon in $\bar{K}^0 \rightarrow \pi^+ e^- \nu$

which gives: $D_{30}=max|S_{30}(t)-F_0(t)|=0.17$

or ~50% probability

The same observations by χ^2 method.

n observations of x belonging to N mutually exclusive classes. $H_0: p_1=p_{01}, p_2=p_{02}, \ldots, p_N=p_{0N}$ for $\Sigma p_{0i}=1$

Test statistic:

$$X^2=\sum_{i=1}^{N}\frac{(n_i-np_{0i})^2}{np_{0i}}=\frac{1}{n}\sum_{i=1}^{N}\frac{n_i^2}{p_{0i}}-n$$

when H_0 is true, this statistic is approximately χ^2 distributed with $N-1$ degrees of freedom.

$\chi^2(obs)=3.0$ with 3 degrees of freedom

or probability of about 0.40

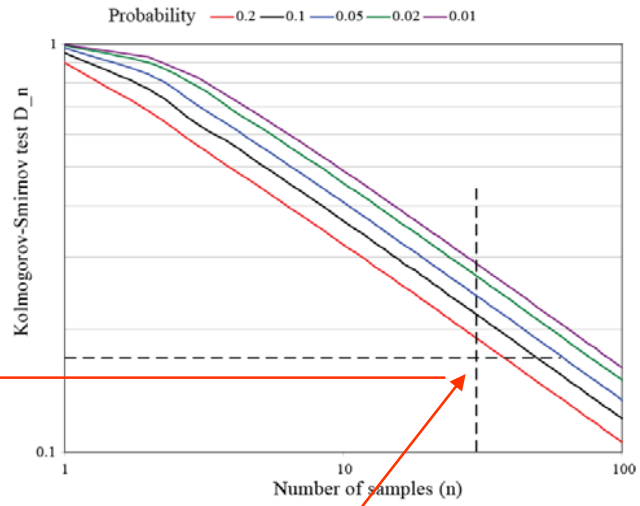

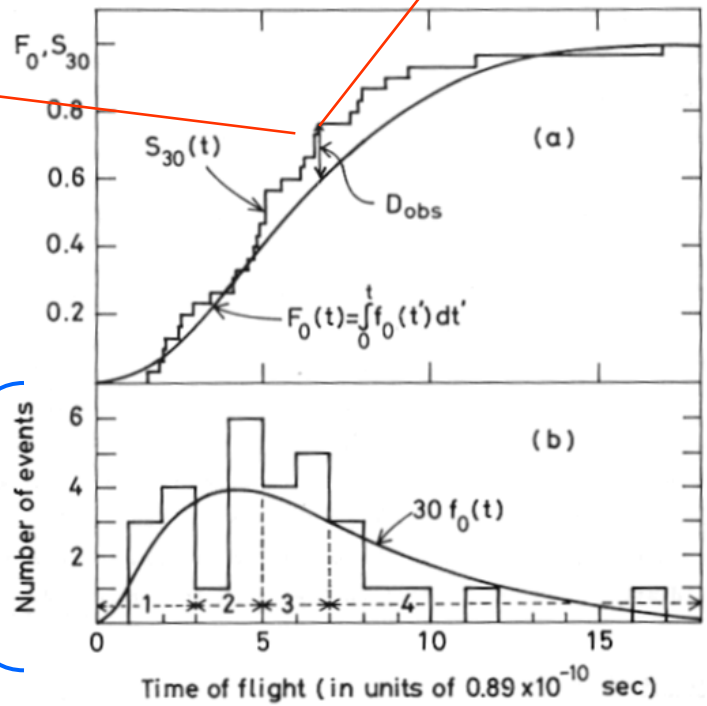

The Hough transform is a technique which can be used to isolate features of a particular shape within an image. The Hough technique is particularly useful for computing a global description of a feature(s) (where the number of solution classes need not be known *a priori*), given (possibly noisy) local measurements. The motivating idea behind the Hough technique for line detection is that each input measurement (*e.g.* coordinate point) indicates its contribution to a globally consistent solution (*e.g.* the physical line which gave rise to that image point).

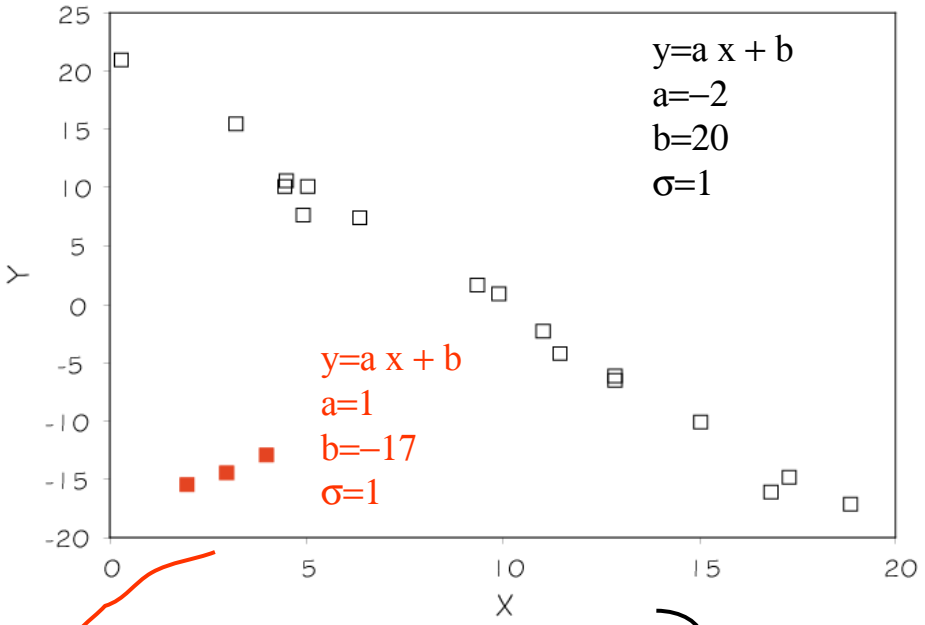

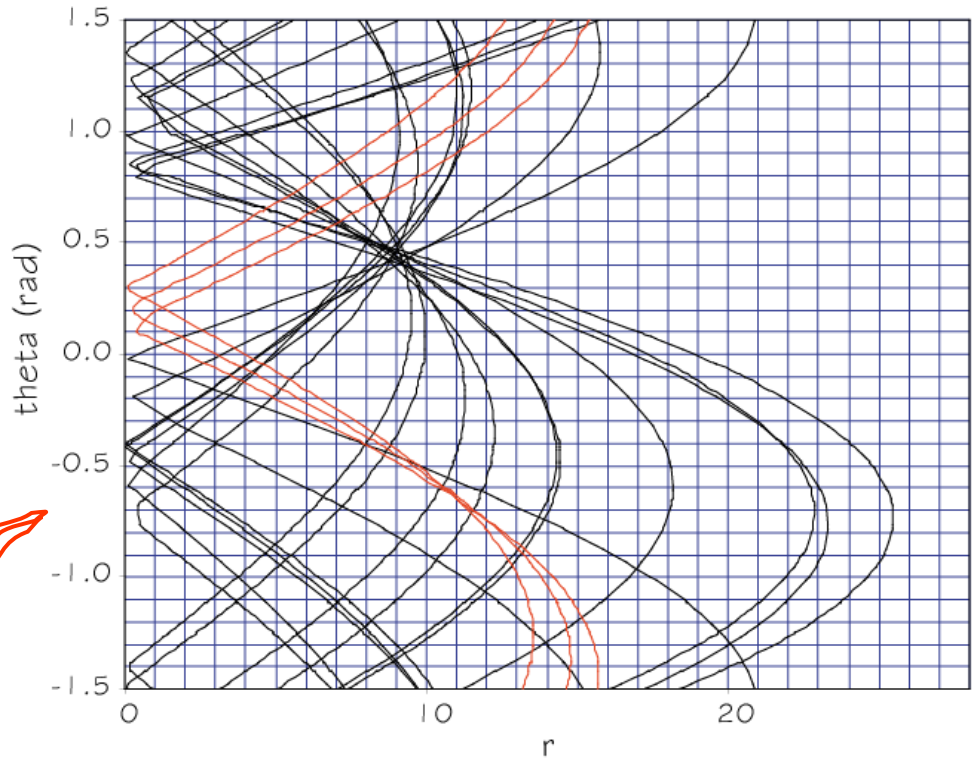

x cosΘ+y sinΘ = r
This *point-to-curve* transformation is the Hough transformation for straight lines

from http://homepages.inf.ed.ac.uk/rbf/HIPR2/hough.htm

Ring Finding with a Markov Chain.

Sample parameter space of ring position and size by use of a Metropolis Metropolis-Hastings Markov Chain Monte Carlo (MCMC)

Interested people should consult:

C.G. Lester, *Trackless ring identification and pattern recognition in Ring Imaging Cherenkov (RICH) detectors*, NIM A 560(2006)621-632

http://lhcb-doc.web.cern.ch/lhcb-doc/presentations/conferencetalks/postscript/2007presentations/G.Wilkinson.pdf

G. Wilkinson, *In search of the rings: Approaches to Cherenkov ring finding and reconstruction in high energy physics*, NIM A 595(2008)228

W. R. Gilks et al., *Markov chain Monte Carlo in practice*, CRC Press, 1996

Example of 100 new rings *proposed* by the "three hit selection method" for consideration by the MHMC for possible inclusion in the final fit. The hits used to seed the proposal rings are visible as small black circles both superimposed on the proposals (left) and on their own (right).

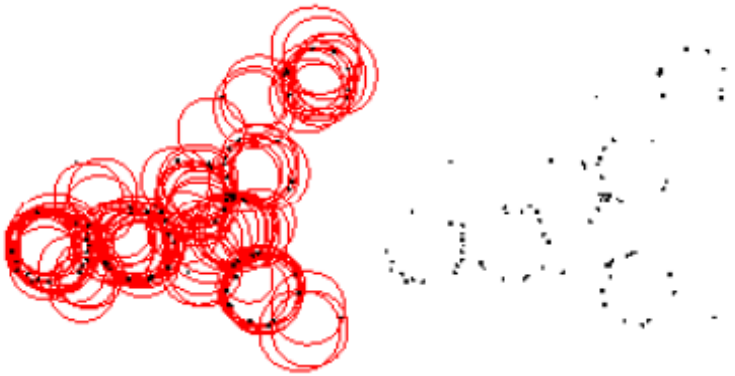

It is not about Markov chain, but have a look in

M.Morháč et al., Application of deconvolution based pattern recognition algorithm for identification of rings in spectra from RICH detectors, Nucl.Instr. and Meth.A(2010),doi:10.1016/j.nima.2010.05.044

Kalman filter

The Kalman filter is a set of mathematical equations that provides an efficient computational (recursive) means to estimate the state of a process, in a way that minimizes the mean of the squared error.
The filter is very powerful in several aspects:
it supports estimations of past, present, and even future states, and it can do so even when the precise nature of the modelled system is unknown.
http://www.cs.unc.edu/~welch/media/pdf/kalman_intro.pdf
iweb.tntech.edu/fhossain/CEE6430/Kalman-filters.ppt

R. Frühwirth, M. Regler (ed), Data analysis techniques for high-energy physics, Cambridge University Press, 2000

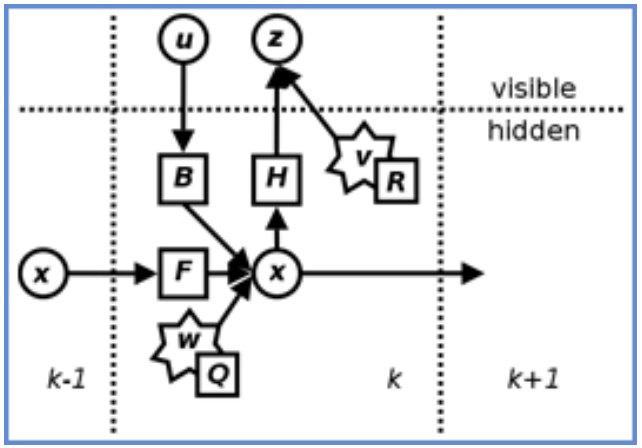

07/10/2009
*US President Barack Obama presents the National Medal of Science to **Rudolf Kalman** of the Swiss Federal Institute of Technology in Zurich during a presentation ceremony for the 2008 National Medal of Science and the National Medal of Technology and Innovation October 7, 2009 in the East Room of the White House in Washington, DC.*
2008
*Academy Fellow **Rudolf Kalman**, Professor Emeritus of the Swiss Federal Institute of Technology in Zurich, has been awarded the Charles Stark Draper Prize by the National Academy of Engineering. The $500,000 annual award is among the engineering profession's highest honors and recognizes engineers whose accomplishments have significantly benefited society. Kalman is honored for "the development and dissemination of the optimal digital technique (known as the Kalman Filter) that is pervasively used to control a vast array of consumer, health, commercial, and defense products."*

Pion-Kaon separation for different PID methods. The length of the detectors needed for 3σ separation.

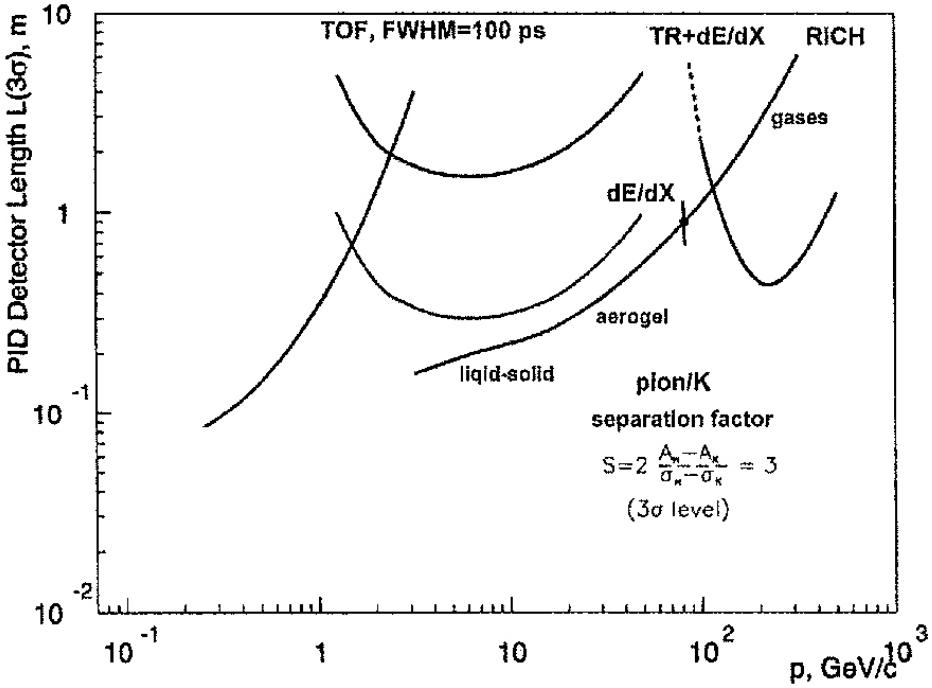

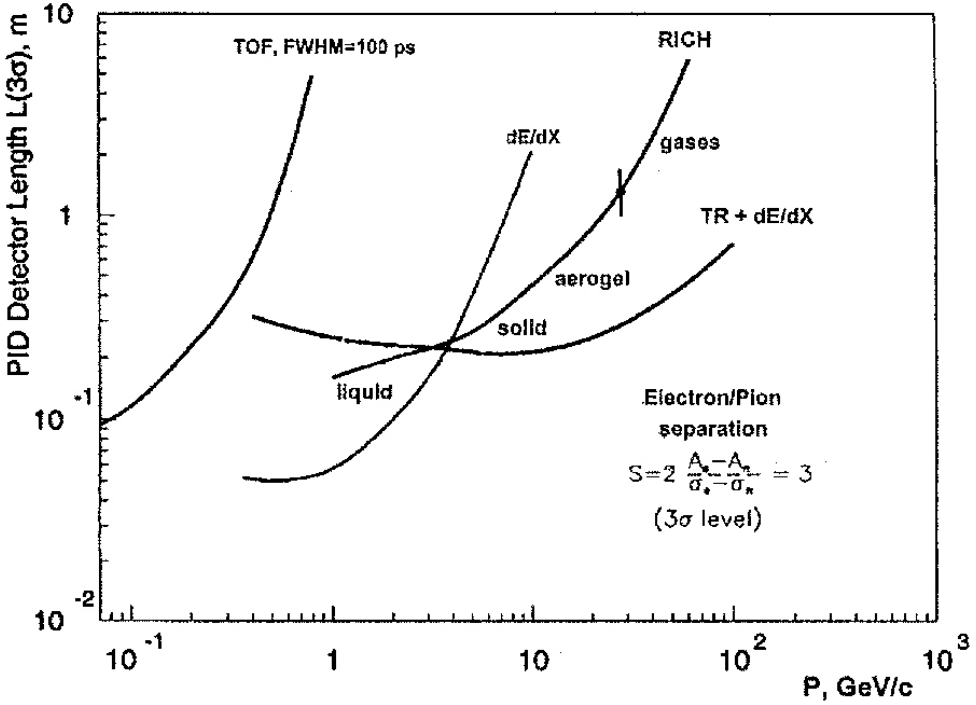

The same as above, but for electron-pion separation.

Dolgoshein, NIM A 433 (1999)